BNL 52082

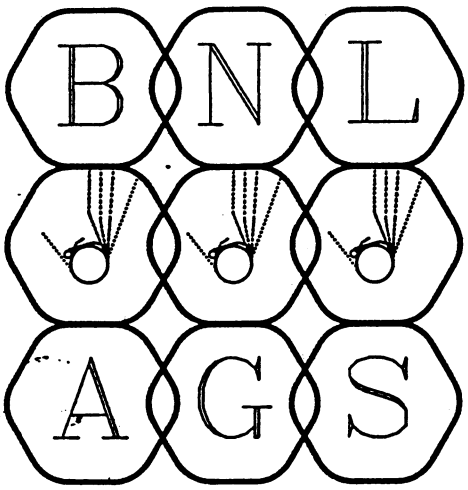

PROCEEDINGS OF THE 1986

SUMMER WORKSHOP ON

ANTIPROTON BEAMS

IN THE 2-10 GeV/c RANGE

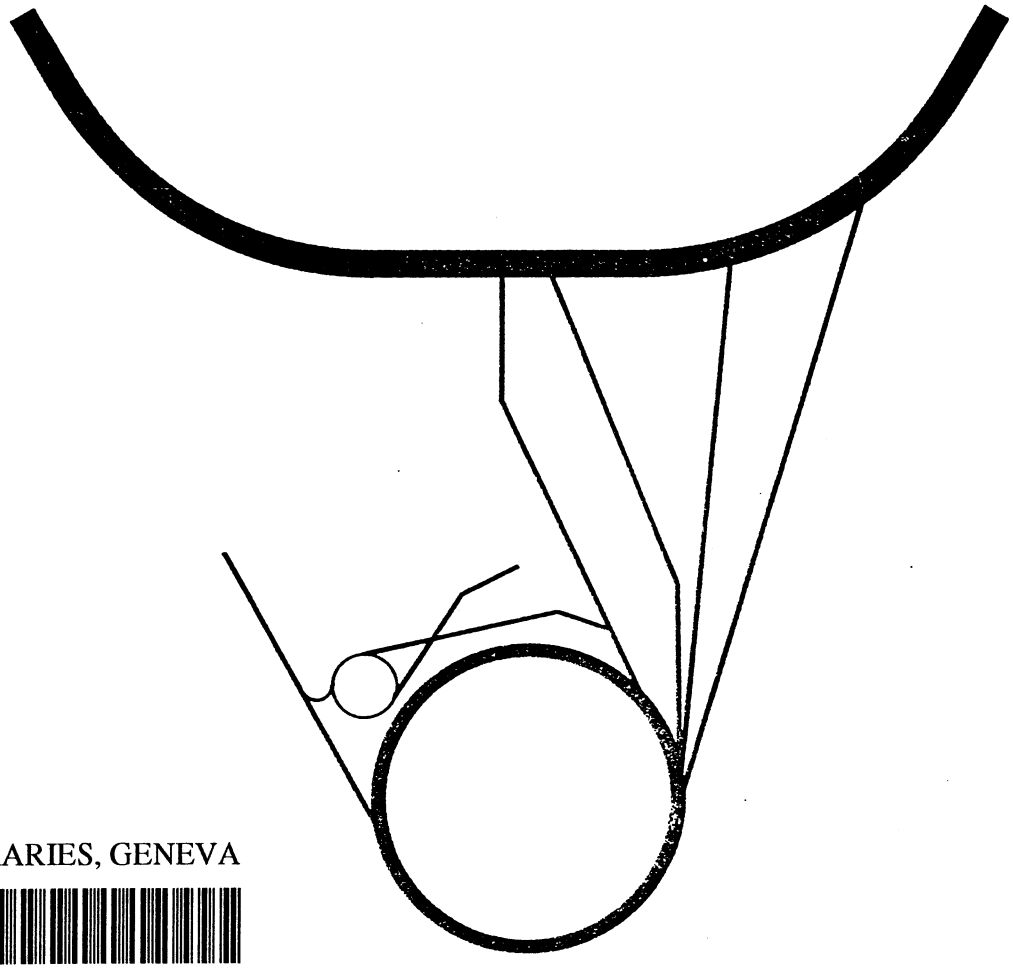

B.E. BONNER - H.N. BROWN - G. BUNCE - A.S. CARROLL - G. DANBY - H.W.J. FOELSCHE - J.W. GLENN III - J. JACKSON - T.E. KALOGEROPOULOS - D.M. LAZARUS - D.M. LEE - Y.Y. LEE - D.I. LOWENSTEIN - G.S. MUTCHLER - D.C. PEASLEE - A.F. PENDZICK - L.S. PINSKY - H. POTH - D.K. ROBINSON

BNL 52082
AGS/EP&S 87-1
UC-28
(Particle Accelerators and
High-Voltage Machines — TIC-4500)

PROCEEDINGS OF THE 1986 SUMMER WORKSHOP ON ANTIPROTON BEAMS IN THE 2-10 GeV/c RANGE

D. Lazarus, Editor

May 7, 1987

AGS DEPARTMENT

BROOKHAVEN NATIONAL LABORATORY
ASSOCIATED UNIVERSITIES, INC.
UPTON, LONG ISLAND, NEW YORK 11973

UNDER CONTRACT NO. DE-AC02-76CH00016 WITH THE
UNITED STATES DEPARTMENT OF ENERGY

Table of Contents

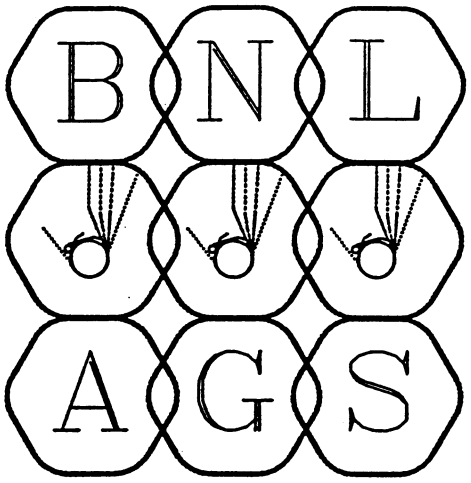

PROCEEDINGS OF THE 1986

SUMMER WORKSHOP ON

ANTIPROTON BEAMS

IN THE 2-10 GeV/c RANGE

B.E. Bonner • Rice University

H.N. Brown • Brookhaven National Laboratory

G. Bunce • Brookhaven National Laboratory

A.S. Carroll • Brookhaven National Laboratory

G. Danby • Brookhaven National Laboratory

H.W.J. Foelsche • Brookhaven National Laboratory

J.W. Glenn, III • Brookhaven National Laboratory

J. Jackson • Brookhaven National Laboratory

T.E. Kalogeropoulos • Syracuse University

D.M. Lazarus • Brookhaven National Laboratory

D.M. Lee • Los Alamos National Laboratory

Y.Y. Lee • Brookhaven National Laboratory

D.I. Lowenstein • Brookhaven National Laboratory

G.S. Mutchler • Rice University

D.C. Peaslee • University of Maryland

A.F. Pendzick • Brookhaven National Laboratory

L.S. Pinsky • University of Houston

H. Poth • Karlsruhe University

D.K. Robinson • Case Western Reserve University

ABSTRACT

The possibilities for building a facility for the formation spectroscopy of "charmonium" and the study of "exotics" at the AGS with high intensity antiproton beams of good resolution and enhanced purity are explored. The performance potential of a number of long beams and the AGS booster are evaluated and costs are estimated. Fluxes of several 10^7 antiprotons per pulse with purities of 5% to 99% are possible with conventional long beams. A similar total antiproton flux would be available with the Booster with no beam contamination. This could effectively be enhanced by two orders of magnitude by reducing the momentum spread in order to scan very narrow (less than 1 MeV) resonances. The maximum momentum attainable with the present Booster magnet design is 5.6 GeV/c which only reaches the $\chi_o(3415)$ charmonium state. Modifications are possible which would raise the maximum momentum to 6.3 GeV/c to include all states up to and including $\eta_c'(3590)$ in its range. The performance potential for this physics at the AGS is found to compare favorably with that at other laboratories with more antiprotons delivered annually, running in the post-Booster era, than at FNAL or Super-Lear with ACOL under typical scheduling conditions. A high resolution purified source of antiprotons in the 2-10 GeV/c range at BNL would cost $3.0M - $4.1M including an experimental hall.

ACKNOWLEDGEMENT

The authors would like to express their gratitude
to Ms. Joan Depken and Mr. Rippie Bouman
for their excellent assistance in preparing these proceedings.

1. INTRODUCTION

Since 1980 there have been several proposals to establish the existence of charmonium states not accessible to formation at electron positron colliders, and to determine their masses and widths. Those states with quantum numbers other than $J^P = 1^-$ -- like the η_c, χ_o, χ_1, χ_2, η_c' and the $^1P_1$ -- can be formed in antiproton-proton collisions. They are of interest because their masses and widths can be calculated from QCD-inspired potentials and a non-relativistic Schroedinger equation with a relatively high degree of confidence, thus providing one of the few quantitative tests of the theory. Gluonic degrees of freedom may lead to additional states beside those derived from simple potentials. The initial proposals SPSC/P81-12 at the CERN SPS, E763 at the AGS, R704 at the ISR, and E792 at the AGS were respectively not approved, withdrawn, approved and run for a limited period (three weeks), and not approved.

The SPS experiment using a one kilometer long beam and a high resolution spectrometer would have been capable of yielding a mass resolution of 300 KeV for the χ states with an antiproton flux of 3×10^6/pulse and $\pi/p = 4.1$ by virtue of the long flight path.

Experiment 763 (LBL/Mt. Holyoke/BNL) was proposed at Brookhaven in 1980 and withdrawn following measurements of the antiproton flux in the Medium Energy Separated Beam. The measured fluxes were 85,000 $\bar{p}$ per 10^{12} protons on target at 3.7 and 6.0 GeV/c. Pion contamination was at the 3:4 and 8:1 level in the two cases. These fluxes were a factor of 3 below those anticipated in the proposal and an order of magnitude less than expectations for R704 at the ISR.

Experiment R704 finally ran as sole user of antiprotons in the ISR with a hydrogen gas jet; in the three week period it was able to obtain data indicating the presence of χ_1, χ_2 and the $^1P_1$ states and to make crude measurements of the widths. The experiment would have been a success had it not been decided to terminate ISR operations. As a result the experiment obtained 30, 50, and 5 events for the respective states above with a mass resolution of about 2 MeV.

Experiment 792, a proposal similar to the SPS experiment, was submitted to the AGS in 1984. In addition to purification by pion decay over a long flight path, a novel feature was put forward in which the beam would be slowly extracted from the AGS while maintaining the rf

bunch structure intact; a total separation of antiprotons and pions in their time of arrival could be made over the long flight path.[1] Although the physics was considered admirable by the Program Committee, the proposal was not approved because of the high cost of the target station, beam, high resolution spectrometer and remote experimental area.

In 1985 some members of the R704 groups plus new collaborators proposed Fermilab E760, an upgraded version of the ISR experiment to run in the Fermilab Antiproton Accumulator during Tevatron fixed target running periods. Improvement by a factor of 5 in intensity and 4 to 5 in detector solid angle was anticipated. The mass resolution in the χ_1, χ_2 region would be 300 KeV. This is to be compared with a resolution of 20 MeV obtained in radiative J/ψ decays by the Crystal Ball collaboration and 2 MeV in R704. Experiment 760 may suffer technical difficulties in decellerating the antiproton beam in the accumulator to the η_c, and J/ψ (an important energy calibration point), but the basic goals can be met. A more serious restriction is the inability to analyze and identify all products of the antiproton-proton interactions over the full solid angle, which is imposed by limited access to and space available in the accumulator ring. This is especially true for the more difficult parts of the experiment where the background may be large or cross section small, as in η_c, $^1D_2$, or $^3D_2$ states.

The sizable community of physicists active in this field held a workshop at Fermilab in April, 1986 and the proceedings[2] provide an excellent summary of the physics potential in this area. Ideally this physics program could best be carried out with the cooled antiproton beam extracted from the Fermilab accumulator and transported to a large solid angle magnetic spectrometer facility providing good particle identification along with good segmentation. In view of the high priority of Tevatron collider experiments CDF and DØ, this is thought to be unlikely.

Because of the great interest in this area of physics and the lack of adequate facilities for this research it was decided to explore the possibilities for a dedicated facility to produce a high intensity purified antiproton beam in the 2-10 GeV/c range at Brookhaven. A workshop was held on August 18-22, 1986, at the AGS Department; several possible options were evaluated, and the results are presented in the following sections.

A new antiproton beam at the AGS should span the range from 2 to 10 GeV/c for the following reasons, in order of ascending momentum:

1. It should connect to the upper momentum of LEAR (2 GeV/c).
2. It should cover the charmonium region.
3. It should reach the $\Lambda_c \bar{\Lambda}_c$ threshold.

The invariant masses of the states in question are given in Table 1-1, along with the corresponding $\bar{p}$ beam momenta required for their formation.

Table 1-1. Charmonium and Hyperon-Antihyperon Masses and Beam Momenta for Formation

Channel	$s^{1/2}$ (MeV)	p(beam)(MeV/c)
$\Sigma^+ - \bar{\Sigma}^+$	2379	1854
$\Sigma^\circ - \bar{\Sigma}^\circ$	2385	1871
$\Sigma^- - \bar{\Sigma}^-$	2395	1899
$\Xi^0 - \bar{\Xi}^0$	2630	2582
$\Xi^- - \bar{\Xi}$	2643	2621
η_c	2980	3689
J/ψ	3097	4066
$\Omega^- - \bar{\Omega}^-$	3345	4936
χ_0	3415	5192
χ_1	3511	5552
$^1P_1$	3525	5607
χ_2	3556	5724
η_c'	3590	5860
$D^+ - \bar{D}^-$	3739	6444
$^3D_1$	3772	6580
$^3D_2/^1D_2$	(3852/3860)*	6910/6940*
$\Lambda_c - \bar{\Lambda}_c$	4562	10109
$\Sigma_c - \bar{\Sigma}_c$	4900	11819

* Predicted

A variety of particle studies is accessible to $\bar{p}$ beams in this energy range: ordinary hadron pairs and their excited states--already observed in e^+e^- collisions[3]--will be much more copious here. Extension of Regge trajectories is facilitated by high initial thresholds, which $\bar{p}p$ provides; and the precise momentum control will enable angular analysis to separate out individual states. Exotics such as the U(3.1) should be readily observed,[4] representing a broad field of study if their existence can be established. There is, in addition, the possibility of charm production in both boson and baryon hosts, but that is the most extreme goal. Although charm may be the most glamorous topic, it may ultimately prove less significant for $\bar{p}p$ pursuit than the larger bulk of other studies outlined above.

As a reference standard the yield of antiprotons measured at CERN has been used.[5] Corrected to AGS operating conditions, this becomes

$$Y = 1.2 \times 10^{-6}\ \bar{p}\ (2\ \text{msr}\ \%\ \text{interacting proton})^{-1} \qquad (1.1)$$

at 5 GeV/c. Equation (1.1) agrees with the Sanford-Wang semiempirical calculation.[6]

For comparison of the various options below, the standard antiproton flux is assumed:

$$F = f\ Y\ \Delta\ \Omega\ \Delta\ p/p = 4.0 \times 10^{-6}\ \bar{p}\ (\text{beam proton})^{-1} \qquad (1.2)$$

where $f \approx 1/3$ is the fraction of beam protons that interact in the target. For the long beam line options the standard assumption is $\Delta\Omega = 5$ msr, $\Delta\ p/p = .04$, which is consistent with the prototype long antiproton beam design of H.N. Brown.[7] The acceptance determined for the booster is $\Delta\Omega = 40$ msr, $\Delta\ p/p = .02$, In order to capture such a large solid angle from the antiproton production target, a lithium lens would be employed with chromatic aberrations that reduce the effective beam proton fraction to $f \approx 1/9$. The lithium lens might also enhance F in other options but is most attractive in the booster option where one would not have to deal with the corresponding increase in pion flux: cf. Table 3-1.

References

1. AGS Experiment 626, T. Kalogeropoulos et al.
2. Proceedings of the First Workshop on Antimatter Physics at Low Energy, April 10-12, 1986. Fermi National Accelerator Laboratory.
3. ARGUS Collaboration, Phys. Lett. 183B, 419 (1987).
4. M. Bourquin et al., Phys. Lett. 172B, 113 (1986).
5. See Appendix 1 for further details.
6. J.R. Sanford and C.L. Wang, BNL 11749 (May, 1979).
7. Included here as Appendix 2.

2. C' TARGET AND 1 KM BEAM

T. Kalogeropoulos, Group Leader
B. Bonner G. Mutchler
H. Brown A. Pendzick
D. Lee K. Robinson

I. Introduction

The primary objective of this group was to reduce the cost of the one kilometer antiproton beam in AGS proposal E792, which is shown in Fig. 2-1. We find that a suitably redesigned beam can be built for about $2.0M plus $0.8M for an experimental area. The cost of the experimental area can be reduced by locating it adjacent to the RHIC open area. This reduces the beam length to 800 meters. These costs do not include the high resolution spectrometer.

II. Beam Characteristics

Table 2-1 summarizes the beam characteristics. All distributions relevant to the beam in E792 apply here. An achievable time-of-flight resolution of δt = 100 psec is assumed. Advantages of this beam design include the following:

1. Compatibility with the SEB program.
2. The muon g-2 ring can be fed from this beam with pion or muon injection.*
3. Construction can start immediately.
4. It does not interfere with RHIC.

A disadvantage is the sacrifice of the LESBII.

Table 2-1. C' BEAM CHARACTERISTICS

Momentum range:	2-11 GeV/c
Momentum bite $\Delta p/p$:	.04
Angular acceptance $\Delta\Omega$:	5 msr
Maximum $\bar{p}$ flux (10^{13} beam prot.)$^{-1}$:	4 x 10^7
Length (meters):	1000 (800)
Purity $\pi^-/\bar{p}$ (5 GeV/c):	7:2 (7:1)
$\bar{p}$ production target location:	C' target moved upstream 6 m
$\bar{p}$ experiment location:	stand-alone hall (RHIC-dependent hall)

* The muon g-2 experiment has been sited elsewhere since the conclusion of the workshop.

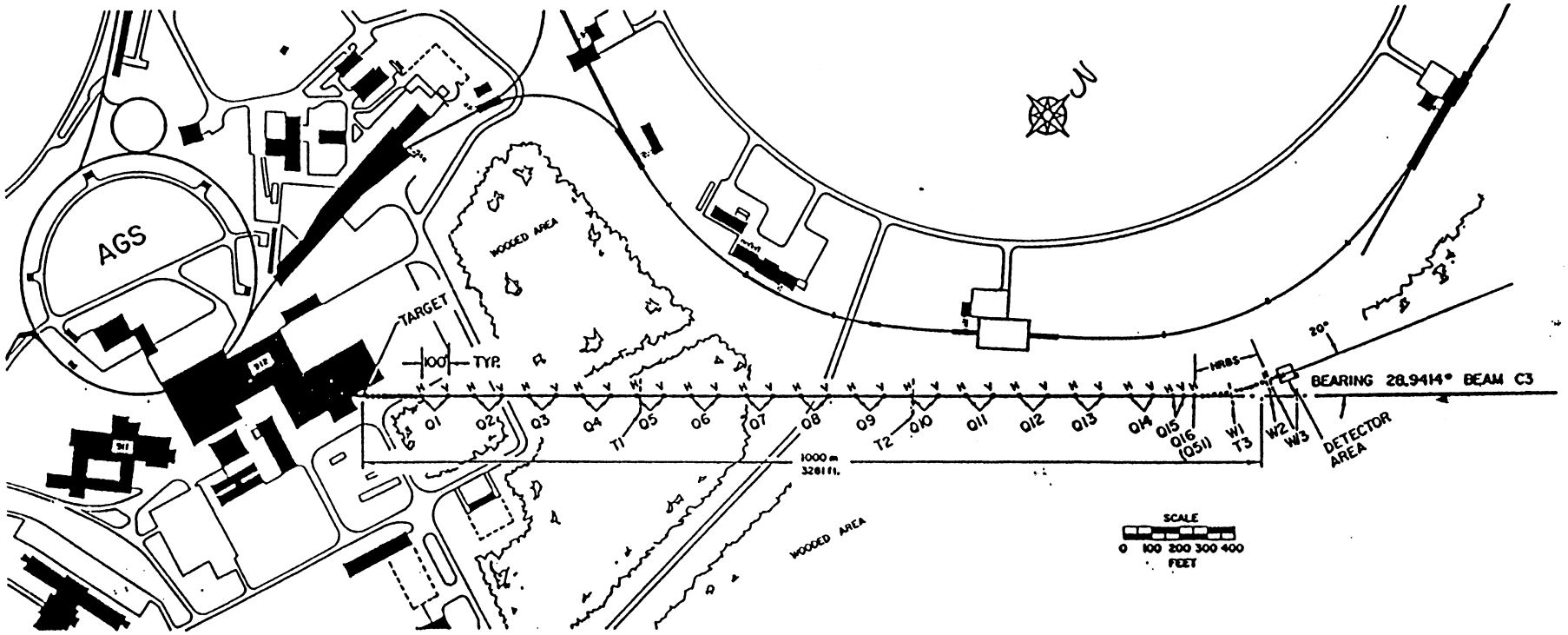

Fig. 2-1. Antiproton C' Line Option

III. Discussion

1. Front Region

In the E792 design the LESBII was unaffected. New shielding and a difficult construction area resulted in $4.0M as a cost estimate. The present recommendation moves the C' target upstream and places the front end (which selects momentum and dumps the primary proton beam) inside the building where all utilities, a crane and the shielding of LESBII are available. In this case the cost is brought down to $825K.

The estimate of $825K includes the cost of 5 quadrupoles at $40K each and 5 dipoles (18D72 or equivalent) at $95K each. This front end for the beam will select momentum bites down to ± 0.3%. The 11 GeV/c momentum covers production of $\Lambda_c \bar{\Lambda}_c$ and $\Sigma_c \bar{\Sigma}_c$ pairs. The dogleg configuration presented in E792 is preferred; another configuration with two dipoles discussed in H. Brown's report (Appendix 2) is also possible and less expensive, but the minimum momentum bit is ± 1%. Such a large minimum is likely to limit the effective luminosity of experiments on narrow charmonium states.

2. Transport Region

The original cost estimate of the beam FODO transport was $1832K. This estimate was made with the beam being built above ground. The cost reduces to $1323K if the beam is trenched in at the AGS beam height.

3. Experimental Area

An experimental area 40'W x 60'L x 30'H can be built at a cost of $755K. The cost can be reduced if this area is close to the RHIC "Open Area" experimental hall where electrical utilities and cooling water are available. In this case the beam length would be 800 meters, and the cost of the experimental area is $430K. This will, in addition, produce a 20% reduction in the cost of the transport.

4. High Resolution Beam Spectrometer (HRBS)

The HRBS allows tagging of antiprotons with a resolution $\Delta p/p = 2 \times 10^{-4}$ with resultant $\bar{p}p$ center-of-mass resolution of about 300 KeV in

the charmonium region. Such resolution is necessary in order to measure widths of narrow ($\lesssim$ 1-2 MeV) states and to reduce associated background. The original cost estimate for this spectrometer amounted to $1660K, half of which was the cost for new 18D72 dipoles or their equivalent.

Considering the Fermilab jet target accumulator experiment (E760) with an expected resolution of 300 KeV/c and the absence of background in $\bar{p}p \to \gamma + J/\psi$ as observed in ISR Experiment R705, the group concluded that the spectrometer is highly desirable. Every effort should be made, moreover, to see whether magnets can be made available rather than relax the resolution and install the HRBS later. It will be more expensive as an add-on.

5. Other Options

The group considered bending the beam by 180° halfway downstream and bringing it back to the LESBII experimental hall. The cost of the 180° bend has been estimated to be about $2.0M. Such a configuration is attractive and offers the possibility of making a storage ring. Because of the cost it has not been pursued further.

IV. Cost Summary

Table 2-2 summarizes the costs of this option. A more detailed breakdown is presented in Appendix 8.

Table 2-2. COST SUMMARY - C' LINE OPTION

	Cost (K$)	Labor (MW)
Proton transport and target region	825	447
Beam transport	1323	627
Experimental area - 1000m	755	25
(800m)	(430)	(25)
TOTAL	2903	1099
	(2578)	(1099)
High Resolution Beam Spectrometer (HRBS)	1070	300

3. SUMMARY OF LONG $\bar{P}$ BEAM IN THE D AND D/U LINES

H. Poth, Group Leader
H. Brown
J. W. Glenn, III
H. Foelsche
D. Lowenstein
A. Pendzick

I. Introduction

This group considered the following possible approaches to a long, decay purified antiproton beam. Their locations are shown in Fig. 3-1.

1. Option U

The production target is installed in the U-line between the 8° and the 10° bends.[1] The captured antiprotons are transported through the RHIC transfer line into the injection area in the RHIC tunnel, deflected upwards to exit the tunnel at ground level, and transported to a new experimental hall next to the compressor building. Requirements include:

i. Installation of a slow extraction system for the U-line from the AGS.
ii. Bypass of the neutrino production target.
iii. Deflection out of the RHIC injection section, $\bar{p}$ transport to the experimental hall.
iv. Cut in the transfer tunnel for shielding.

2. Option D/U

The production target is installed in the D-line as far upstream as possible.. From there the $\bar{p}$ beam is bent 30° into the AGS tunnel and transported to the U-line with which it is merged shortly behind the U-line extraction point from the AGS at H10. The rest is equivalent to the previous option. This lengthens the beam by about 200 meters. Requirements include:

i. Beam transport from the production area to the RHIC transfer line.
ii. Deflection out of the RHIC injection section, $\bar{p}$ beam transport to the experimental hall.

3. Option D/(g-2) *

Here a production target in the D-line is also used as a pion production target for the muon g-2 experiment. Downstream of the target and the first quadrupoles is a switch magnet that serves either the g-2 ring or the $\bar{p}$ beam. From the switch magnet there follows a straight $\bar{p}$ beam transport to the injection section of RHIC, where a separate experimental hall is needed.

4. Option D/(g-2)' *

The same front end as for D/(g-2) is followed by an additional 20° bend at the end of the parking area. This directs the beam to the RHIC wide angle hall, which is used as the experimental hall for $\bar{p}$ experiments. Requirements include beams transport from the production target to the experimental hall.

II. Beam Characteristics

The $\bar{p}$ beams of this section are listed in Table 3-1. The acceptance of the U-line is restricted; this is slightly ameliorated when the U-target station is used because of better beam focus. As one can see from the table, the beam properties do not differ very much. Whatever option is considered, the requirements for the following items are practically invariant:

1. Proton beam focus on the production target.
2. $\bar{p}$ production target and shielding.
3. $\bar{p}$ capture into transfer line.
4. Experimental hall.

Further remarks on the features of conventional antiproton beams can be found in Appendix 3.

III. Discussion

One should note the importance of small beam emittance if one wants to momentum analyze the antiproton beam or use a long target of small diameter. Moreover, low emittance facilitates the use of a beam separator. The

* The muon g-2 experiment has been sited elsewhere since the conclusion of the workshop.

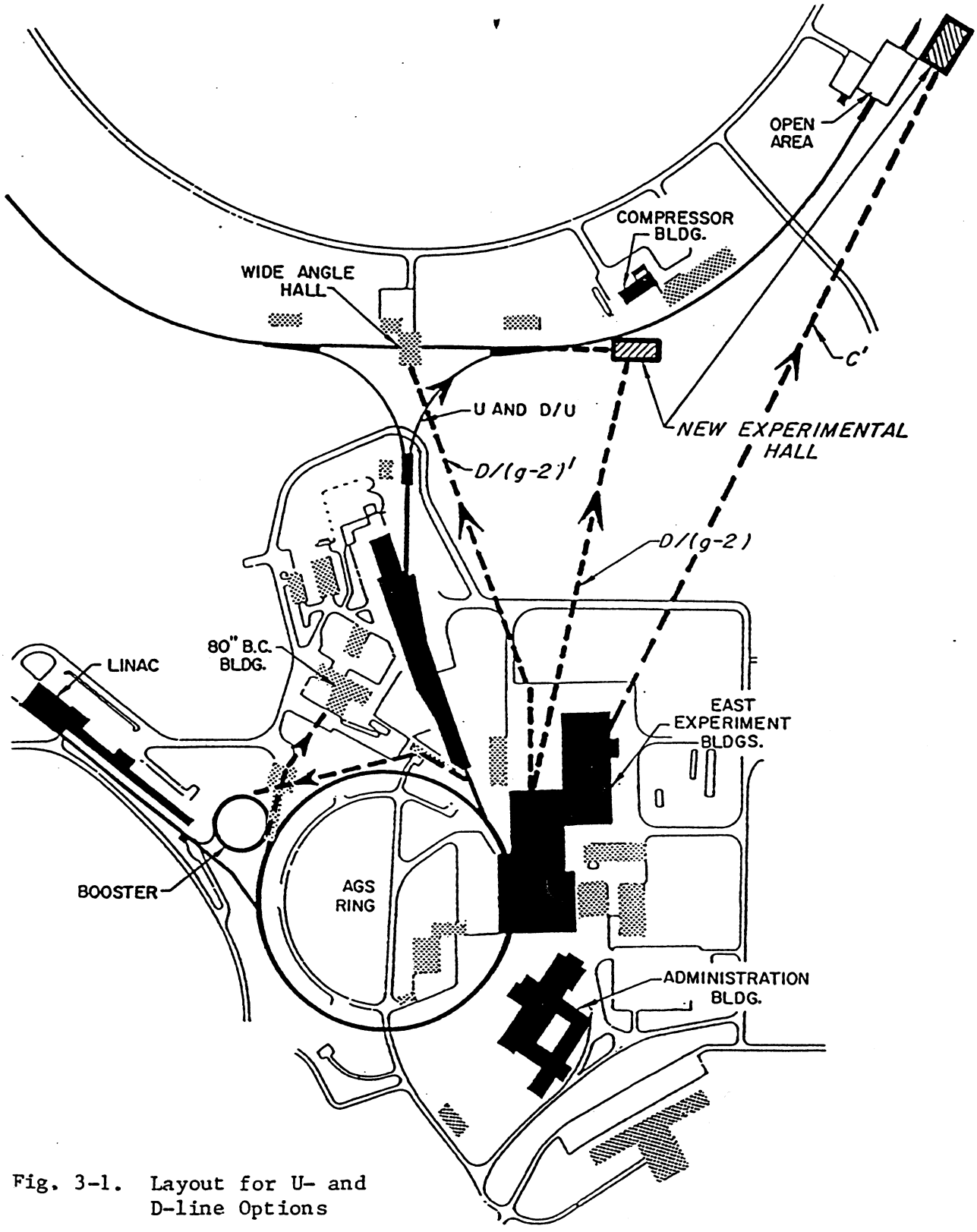

Fig. 3-1. Layout for U- and D-line Options

Table 3-1. U AND D LINE BEAM CHARACTERISTICS

Options:	U-line	D/U line	D/(g-2)	D/(g-2)'
Momentum range (GeV/c):	2 - 10	2 - 10	2 - 10	2 - 10
Momentum bite $\Delta p/p$:	.02	.02	.04	.04
Angular acceptance $\Delta\Omega$ (msr):	*1.7	*0.8	**7	**7
Maximum $\bar{p}$ flux $(10^{13}$ beam prot.$)^{-1}$:	0.7×10^7	0.3×10^7	5×10^7	5×10^7
Purity $\pi^-/\bar{p}$ (5 GeV/c):	14:1	7:1	21:1	14:1
Length (meters):	500	700	600	650
$\bar{p}$ production location:	U target	D target	D target	D target
$\bar{p}$ experiment location:	New hall near RHIC compressor building - - - - -			RHIC wide angle hal

* Special restrictions of U-line, combined with improved focus at U production target.

** To fill the angular acceptance of 20 msr will require a lithium lens, which introduces a chromatic aberration loss factor of about 1/3: hence a net effective solid angle of 20 x (1/3) ≈ 7 msr. See Appendix 6 for the same considerations applied to the booster option.

beam length is of importance mostly at higher momenta, since for a length below 1 km, the decay purification is not very good and the π-$\bar{p}$ flight time difference does not allow an effective separation. At 4 GeV/c and below, however, a beam length of 600m should suffice.

From experimental considerations, it is apparent that we should examine in more detail how to get rid of other negative particles (electrons, muons, pions) in the beam. They cause high accidental rates in detectors, in particular beam time-of-flight counters, and ultimately limit the rate at which an experiment can run. Not all possibilities were checked in detail, but there are essentially three ways to achieve greater purity of $\bar{p}$ beams:

1. A fast kicker near the end of the beam line.
2. An rf separated beam using one separator.
3. A two rf separator beam.

The first two methods require bunched extraction from the AGS. While a fast kicker could do the job in a long line (perhaps by installing it at the vertical bend in the RHIC injection station for options U and D/U), the use of rf separators would render a long antiproton beam unnecessary. The use of two rf separators at high frequency -- e.g., 2.9 GHz -- with slow extraction of a debunched beam would be compatible with the rest of the program. This would avoid the poor duty cycle that would result with bunching at the AGS frequency. This possibility should be considered in the future in more detail.

With respect to the future extension of a long antiproton beam line, options U, D/U, and D/(g-2)' provide the possibility of injecting the antiproton beam into RHIC and transporting it to any desired experimental area. Hence the beam length can be extended considerably. What might be even more interesting in this respect is the possible "loan" of a sophisticated RHIC detector for an antiproton experiment.

In summary, none of the options has an outstanding advantage over the others, and different criteria have to be found to select the right option. Cost and compatibility with the rest of the program are most important.

IV. Cost Summaries

Table 3-2 contains cost summaries for the various options in comparative form. A more detailed breakdown is presented in Appendix 8.

References

1. H. Poth, "A New Approach to a Pure Antiproton Beam at GeV Energies", BNL EP&S Tech. Note 110 (May 1985); also presented at Brookhaven HEDG meeting in April 1986.

Table 3-2. COST SUMMARIES - LONG $\bar{P}$ BEAM STUDIES

Options:	U-line		D/U-line		D/(g-2)		D/(g-2)'	
	Cost (K$)	Labor (MW)	Cost (K$)	Labor (MW)	Cost (K$)	Labor (MW)	Cost (K$)	Labor (MW)
Extraction system	500	186						
Proton transport	155	83	190	26	190	62	190	62
Target region	1105	113	650	228	275	119	275	119
Beam transport	1130	364	1865	656	724	309	1348	486
Experimental area	455	25	455	25	455	25		
Totals	3345	771	3160	935	1644	515	1813	667

4. ANTIPROTON BEAMS FROM THE BOOSTER

A.S. Carroll, Group Leader
Y.Y. Lee
D.C. Peaslee
A.L. Pendzick
L.S. Pinsky

I. Introduction

The concept is outlined in Fig. 4-1. In each AGS cycle the booster is filled with protons and operates normally, ejecting into the AGS. After acceleration in the AGS, fast extraction of 3 rf beam bunches occurs at H10 into the U-line where they are focused on an antiproton production target. The remaining 9 AGS bunches are available for other purposes. The antiprotons are collected by a lithium lens and transported at 4 GeV/c, near peak production, to the booster where they are injected through the proton extraction channel, running in reverse direction around the booster. They are then extracted in one straight section with a moderately thick septum tangent to the AGS and transported directly to the 80-inch bubble chamber complex, which serves as an experimental area.* The extraction and transport occurs during the AGS spill. The booster is then ready to accept the next charge of protons at the usual repetition rate.

II. Beam Characteristics

Table 4-1 summarizes the beam characteristics which are further explained in the following paragraphs.

The booster magnet system as presently designed can reach an antiproton momentum of 5.2 GeV/c at 12.7 kg corresponding to a center-of-mass energy in $\bar{p}p$ collisions of $s^{1/2} = 3.42$ GeV. This would allow formation of $\eta_c(2980)$, $J/\psi(3100)$, and $\chi_0(3415)$ but nothing higher in the hidden charm sequence. A more desirable limit physically is $s^{1/2} = 3.70$ GeV, corresponding to a $\bar{p}$ momentum of 6.3 GeV/c, which would allow production of $\psi'(3685)$, $\eta_c'(3590)$ and all the χ states. More detailed studies in Appendix 5 address the feasibility of such an extension in momentum range.

* The 80-inch bubble chamber building has been chosen as the Experimental Hall for the muon g-2 experiment since the time of the workshop.

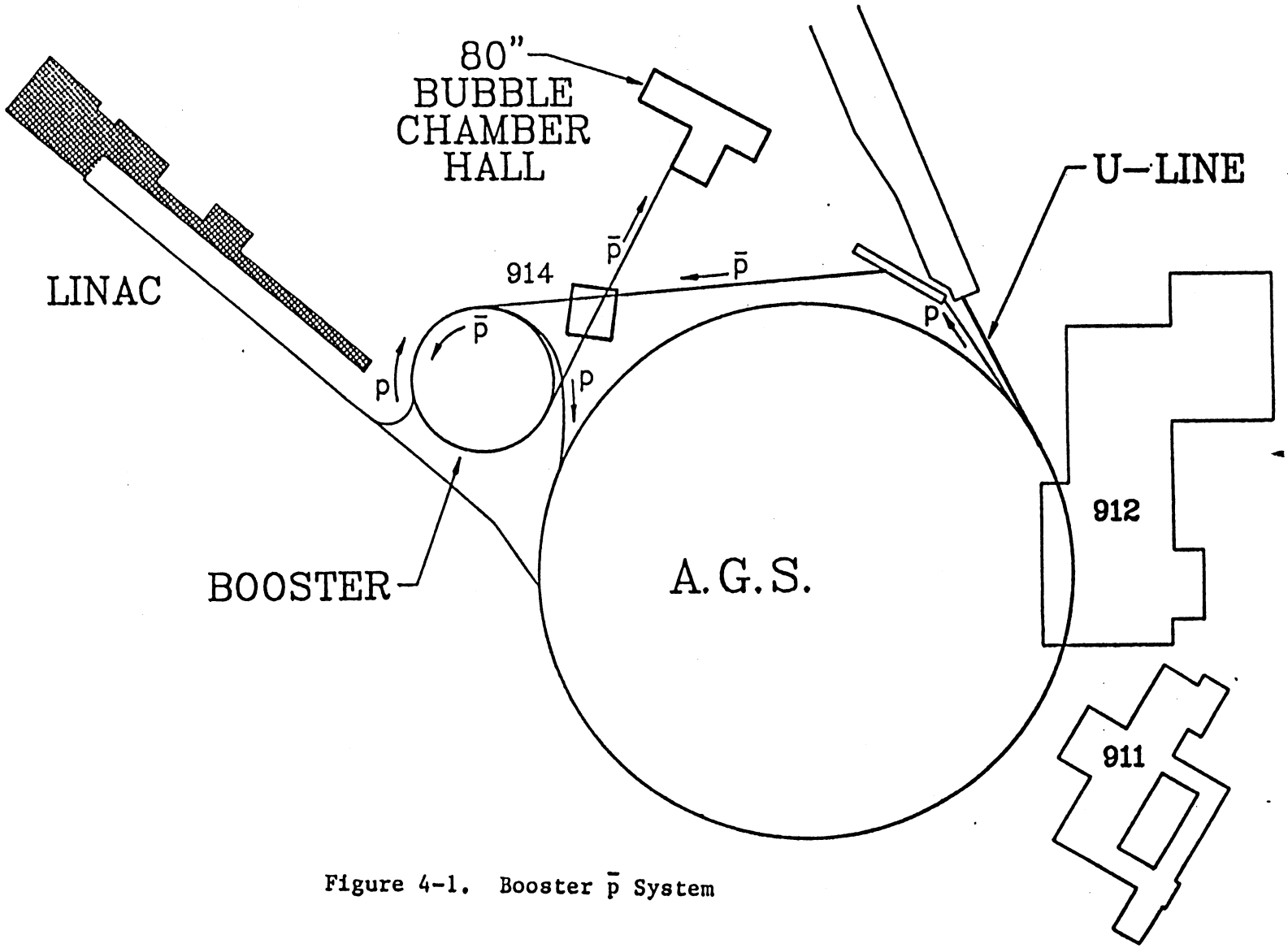

Figure 4-1. Booster $\bar{p}$ System

Table 4-1. BOOSTER ANTIPROTON BEAM CHARACTERISTICS

Momentum range:	0.65 - 5.2 GeV/c
Momentum acceptance $\Delta p/p$:	.02
Angular acceptance:	40 msr
Maximum $\bar{p}$ flux $(10^{13}$ beam prot.$)^{-1}$:	4×10^{7}
Purity $\pi^-/\bar{p}$ (all momenta):	0:1
Length (meters):	(not relevant)
$\bar{p}$ production target location:	U-line target
Experimental Area:	80" bubble chamber bldg.*

The momentum spread of ±1% delivered from the $\bar{p}$ production target can be reduced to $\sim 10^{-4}$ by debunching, and further by phase displacement acceleration during extraction. It is important to note that this procedure compresses the Δp of the total $\bar{p}$ flux without loss of particles; a double advantage results--wide Δp for search and scan, narrow Δp for study of a resonance already located.

The purity of the extracted $\bar{p}$ beam is essentially perfect, since the booster ring functions as an extremely long beam line with very large dispersion.

The muon g-2 experiment can use the same target and experimental area. Since both $\bar{p}$'s in the booster and g-2 require fast extraction and there are no slow extraction requirements in the U-line, the compatibility may be better than in other lines such as C' and D where experiments requiring slow extraction are also mounted.

The availability of antiprotons from this system must wait on completion and commissioning of the booster. Under ideal conditions this could occur as early as 1990, but it seems more realistic to allow early 1991 as the initial date likely for antiproton experiments. Of course the target and direct beam line to the experimental area can be built at once and used for antiproton and muon g-2 studies.

The cost estimate for 5.2 GeV/c antiprotons is detailed in Table 4-2 and includes all necessary modifications to the booster itself, as well as the extra costs of going to 6.3 GeV/c.

* The 80" Bubble Chamber building has been chosen for the muon g-2 experimental area since the conclusion of the Workshop. An extension to this building would provide an ideal experimental area at low cost by utilizing existing services.

III. Discussion

1. Advantages

The specifications above already display some of the advantages of this concept, but it may be worthwhile to recount a more complete list:

i. Pure $\bar{p}$ beam with no muon halo.
ii. High flux, $\bar{p}$'s always taken at production maximum.
iii. High resolution (10^{-4}) without additional means such as HRBS.
iv. Momentum compression with existing booster rf.
v. Continuously tunable momentum.
vi. Well equipped experimental hall immediately available.*
vii. Compatible with AGS slowly extracted beam (SEB) operation.
viii. Nearly ideal compatibility with muon g-2 experiment.
ix. Very flat spill, booster acts as $\bar{p}$ stretcher.
x. $\bar{d}$ beams available without modification.
xi. Very low momentum antiprotons also possible (cf. Appendix 6).

2. Disadvantages

The principal drawbacks of this scheme are as follows:

i. The time before availability is approximately 4 years.
ii. The maximum momentum $\bar{p} \lesssim 5.2$ GeV/c with the present booster design.

If the present concept appears viable, it will be necessary to make immediate plans for adapting the booster as described, in order to incorporate the needed changes in construction.

IV. Cost Summary

The cost summary in Table 4-2 assumes the use of the present H10 extraction system and of all shielding in the proton target area already provided for the muon g-2 experiment, as well as the same target. If it should not prove possible to use the same target, the booster option must

* The 80-inch bubble chamber building has been chosen as the Experimental Hall for the muon g-2 experiment since the time of the workshop.

include the cost of a primary target station, which is included as a contingency. If, however, the preferred extraction for g-2 is at I-10 then locating there would effect savings in the $\bar{p}$ transport line and bending magnets.* A more detailed breakdown is presented in Appendix 8.

The preliminary cost estimate of \$3.6M is on the same order as any other scheme that produces $\bar{p}$ beams of comparable flux, purity, resolution and controllability.

Table 4-2. COST SUMMARY - BOOSTER OPTION

	Cost (K\$)	Labor (MW)
Target region	945	123
50° bend and $\bar{p}$ transport to booster	1016	378
Booster magnet modifications to reach 6.3 GeV/c	990	284
Transport to 80" bubble chamber **	626	175
Experimental area	430	25
TOTAL	4107	985

* I-10 has been chosen for extraction to a target for the muon g-2 experiment since the conclusion of the workshop.

** The 80" Bubble Chamber building has been chosen for the muon g-2 experimental area since the conclusion of the Workshop. An extension to this building would provide an experimental area at low cost by utilizing existing services.

5. CONCLUSIONS

The highest performance option for a purified intense antiproton beam at the AGS would clearly be the booster option if not for the limited momentum range. The ability to vary the momentum spread is a unique and powerful tool for formation spectroscopy. Once a given state has been located in a scan with a relatively large momentum bite e.g. $\frac{\Delta p}{p}$ = .02, the bite could then be reduced to scan an object of width less than 1 MeV. This amounts to an increase in effective luminosity by the same two orders of magnitude. This would not be possible in the long beam options. Unfortunately the top momentum of 6.3 GeV/c would not permit formation of the $^1D_2$ and $^3D_2$ states. The economic and political aspects of further modifying the booster design at this stage would weigh heavily on this option.

The long flight path beams are in general not terribly different from one another in performance or cost. The most attractive is the beam from the C' target area to a new area adjacent to the RHIC Open Experimental Area. It is the longest beam and would deliver antiprotons to a "bargain" experimental hall, which would obtain power and water from the Open Area Hall. The other long beam options suffer somewhat in their shorter lengths and compromises with other installations such as the neutrino area and RHIC injection and experimental areas.

The high resolution spectrometer would be necessary for any of these beam line options to be competitive in the measurement of widths of charmonium states. At best, time-of-flight can yield resolutions approaching 2 MeV in the center-of-mass, even if one ignores the very high rates in the beam counter hodoscopes due to more than 10^8 beam pions per spill.

The momentum resolution is plotted as a function of momentum, for each of the beams under consideration, in Fig. 5-1. A similar plot for the center-of-mass resolution is given in Fig. 5-2.

Table 5-1 compares costs of all the schemes considered here.

Table 5-1. OVERALL COST SUMMARY

	Cost (M$)	Labor (MW)
C' Option	2.90	1099
(with inexpensive hall)	(2.58)	(1099)
U-line Option	3.16	771
D/U-line Option	2.60	757
D/(g-2) Option	1.64	515
D/(g-2)' Option	1.81	667
High Resolution Beam Spectrometer for above	1.07	300
Booster Option	4.11	985

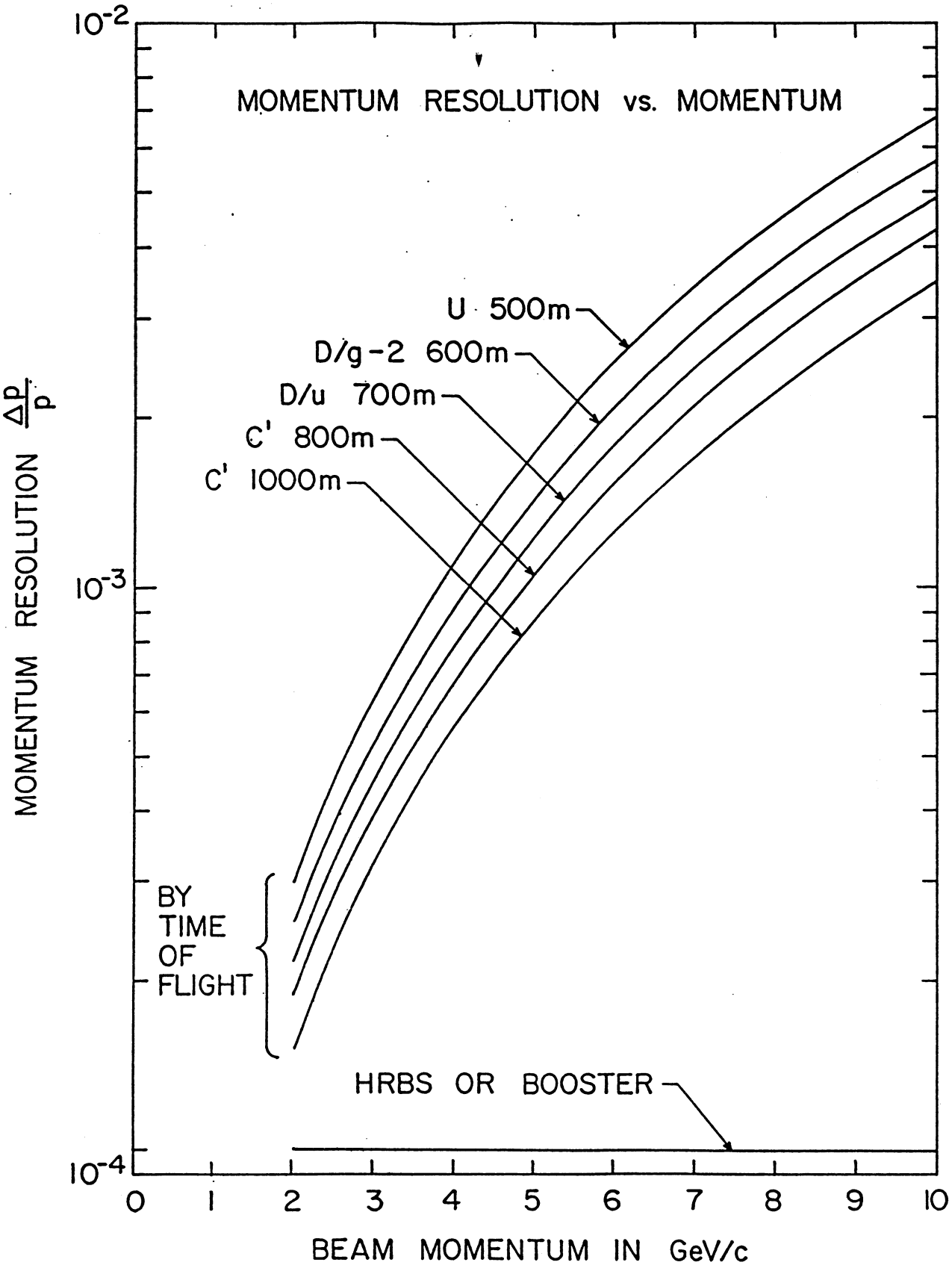

Fig. 5-1. Momentum resolution for the various beam options.

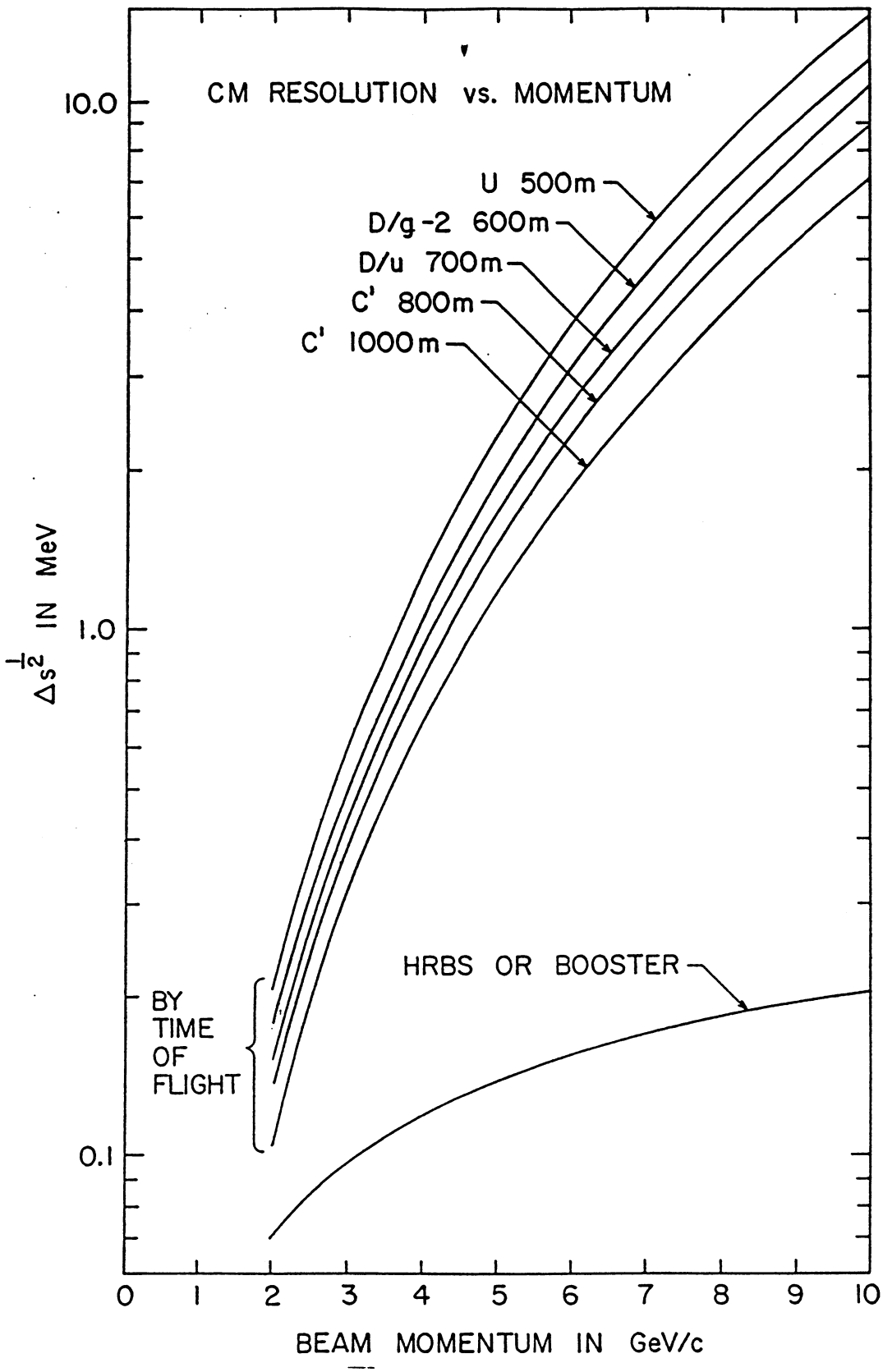

Fig. 5-2. Center-of-mass resolution for the various options.

APPENDIX 1. Antiproton Production Spectra

D. M. Lazarus

I. CERN Results

The antiproton production originally assumed[1] in the design of the CERN Antiproton Accumulator (AA) was $d\sigma_0 = 2.46 \pm 0.42 \times 10^{-2}$ $\bar{p}$ (sr GeV/c interacting proton)$^{-1}$ based on measurements[2] with 23 GeV/c protons on a Pb target on a supposed spectral maximum for antiprotons of 4 GeV/c. The antiproton flux measured at the AA was a factor 3-4 lower than anticipated.[3] The production cross section was accordingly reduced by a factor of 2. The numerical value for the yield is then

$$Y = 2 \times 10^{-2} \times 4 \times d\sigma \qquad \text{(A1.1)}$$
$$= 0.98 \pm 0.17 \times 10^{-6}\ \bar{p}\ \text{(2 msr \%-interacting proton)}^{-1}.$$

for production of 4 GeV/c antiprotons by 23 GeV/c protons.

To scale to AGS operating conditions, we use the Sanford-Wang formula[4] for the increase of primary energy to 28.3 GeV, and to account for peak production momentum of 5 GeV/c instead of 4 GeV/c. Thus,

$$Y_A = 1.2 \pm 0.2 \times 10^{-6}\ \text{(2 msr \% interacting protons)}^{-1} \qquad \text{(A1.2)}$$

which appears as Eq. (1.1) in the text. No correction for target material is made.

II. Sanford-Wang Formulas

The yield predicted by Sanford-Wang formulas for antiproton production[4] from 28.3 GeV protons on Be is shown in Fig. A1-1, averaged over two different solid angles about 0°: 5 msr and 40 msr. The first is appropriate to long beam line options, the second to the booster. The 5 msr curve has a broad maximum between $\bar{p}$ momenta of 5 and 6 GeV/c at $Y = 1.3 \times 10^{-6}$, the 40 msr curve peaks at 4-5 GeV/c with a maximum $Y = 0.9 \times 10^{-6}$. The difference arises from greater weighting of wide-angle production in the second case.

To convert to anticipated $\bar{p}$ flux, we assume f = 1/3 as the fraction of beam protons that interact in the production target. Hence for beam

line options with $\Delta\Omega$ = 5 msr and $\Delta p/p$ = .04 the peak flux is

$$F = f\ Y\ \Delta\Omega\ \Delta p/p = (1/3) \times 1.2 \times 10^{-6} \times 5 \times 2$$
$$= 4 \times 10^{-6}\ \bar{p}\ (\text{beam proton})^{-1} \qquad \text{(A1.3)}$$

For the booster option, chromatic aberrations in the lithium lens induce a further reduction in f by a factor 3: namely, f = 1/9. Then with $\Delta\Omega$ = 40 msr and $\Delta p/p$ = .02 the peak flux becomes

$$F = (1/9) \times 0.9 \times 10^{-6} \times 40 \times 1 = 4 \times 10^{-6}\ \bar{p}\ (\text{beam proton})^{-1} \qquad \text{(A1.4)}$$

This is the same number as in Eq. (A1.3) and is adopted in Eq. (1.2) of the text.

III. AGS Medium Energy Separated Beam (MESB)

The MESB[5] at the Brookhaven AGS has a calculated acceptance of $\Delta\Omega$ $\Delta p/p$ = 0.3 x 6 = 0.9 msr % and a production angle of 3°. At both 3.7 and 6 GeV/c the Sanford-Wang prediction is $2 \times 10^5\ \bar{p}$ $(10^{12}$ beam protons$)^{-1}$. The measured values[6] are 0.9×10^5 and $.85 \times 10^5$ with $\pi/p \approx 3{:}4$ and 8:1

ratios respectively. This flux is more than a factor 2 lower than expected. It is possible that the mass slit and momentum jaws were not adjusted to full beam acceptance because of the high degree of pion contamination.

References

1. "Design Study of a Proton-Antiproton Colliding Beam Facility," CERN/PS/AA/78-3.

2. D. Dekkers et al., Phys. Rev. 137, B962 (1965).

3. E. Jones et al., IEEE Trans. Nuc. Sci. 30, 2778 (1983).

4. J.R. Sanford and C.L. Wang, BNL 11479 (May, 1967).

5. C.T. Murphy and J.D. Fox, BNL 18627 (January, 1974).

6. Brookhaven E763 internal memorandum (March, 1981).

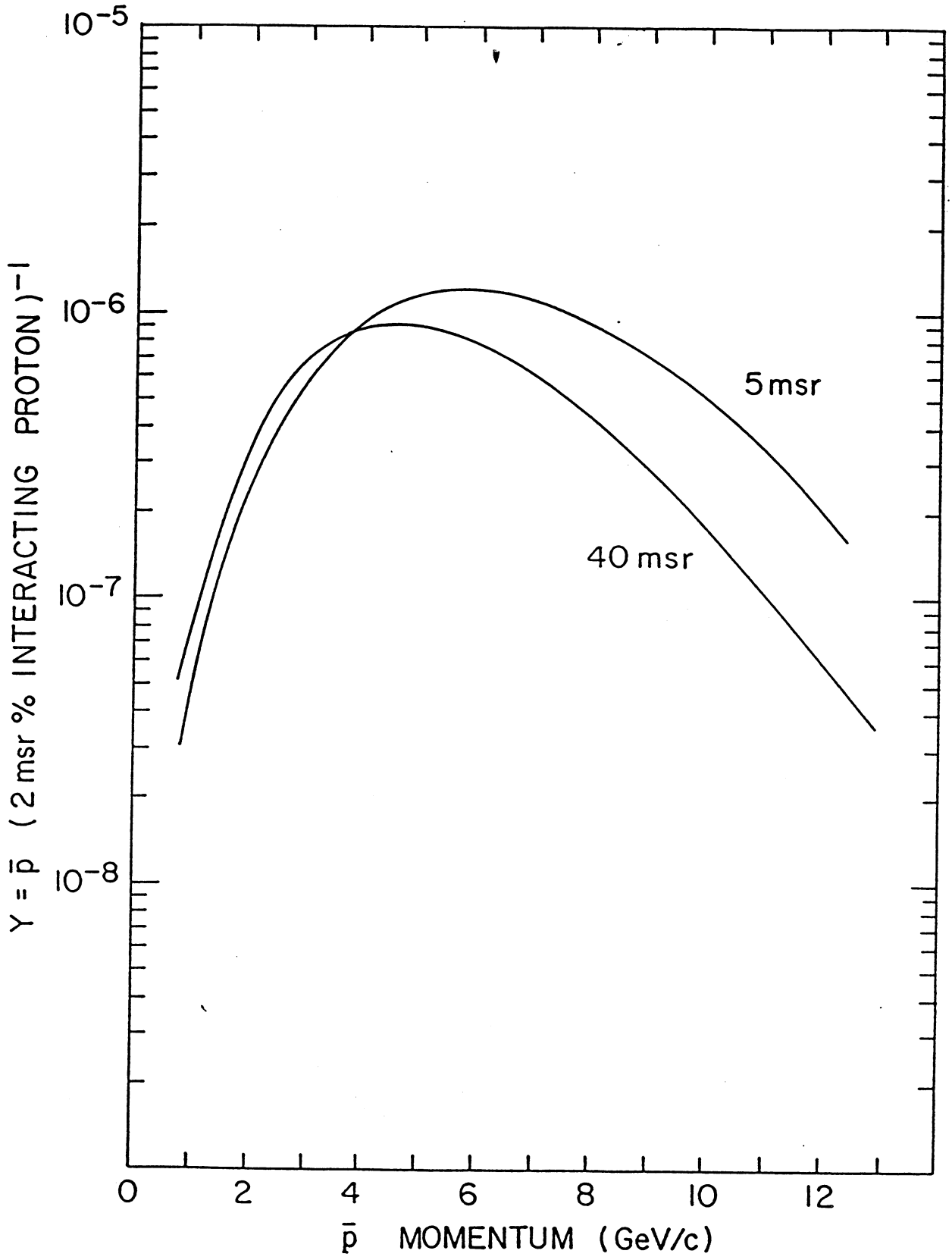

Fig. Al.1. Antiproton yield for 28.3 GeV/c protons on Be

APPENDIX 2. A Time Separated $\bar{p}$ Beam

H. N. Brown

Accelerator Department

BROOKHAVEN NATIONAL LABORATORY
Associated Universities, Inc.

EP&S DIVISION TECHNICAL NOTE

NO. 90

H. Brown

June 2, 1980

A TIME SEPARATED $\bar{p}$ BEAM

This was originally issued as BNL EP&S Division Technical Note No. 90, June 1, 1980. It is reproduced here in its original form.

A Time Separated $\bar{p}$ Beam

I. Introduction

In 1974, Fainberg and Kalogeropoulos[1] measured the time structure of a resonant extracted beam from the AGS with the RF kept on to maintain tight bunching. The external pulses were found to be unexpectedly narrow (FWHM = 2.4 nsec after correction for counter resolution). An explanation for this and some pertinent comments were put forth by Barton[2] in a subsequent report.

The original motivation for the study was to examine the extent to which single counter time of flight (TOF) measurements would be feasible, making it possible to measure velocities of neutral secondary particles from a target.[3] The encouraging result led later to a proposal by Kalogeropoulos[4] to use the tightly bunched protons to produce a secondary time separated beam (TSB) of anti-protons, i.e., a beam with a long flight path over which the lower velocity particles ($\bar{p}$'s) separate longitudinally from the more numberous fast particles (π's) so that the $\bar{p}$ interactions can be studied independently by suitably gated detectors.

II. TOF Characteristics

For a given beam length L, there are various momenta p at which the $\bar{p}$ TOF is equal to the π^- TOF plus an integral number of AGS bunch periods:

$$t_{\bar{p}} = t_{\pi} + n\,T$$

i.e., $\bar{p}$'s of these flight times are overlapped by the intense π^- bursts from later bunches striking the target. If the effective π^- pulse width is $\pm\,\delta$, then there are overlap bands given by

$$\Delta(p,L) \equiv (t_{\bar{p}} - t_{\pi}) = n\,T \pm \delta \qquad (1)$$

within which beam particles are unusable and the experimental detectors are to be vetoed. For n = 0, only $\Delta = +\delta$ has significance. The function Δ is:

$$\Delta(p,L) = \frac{L}{c}\left(\frac{1}{\beta_{\bar{p}}} - \frac{1}{\beta_{\pi^-}}\right) = \frac{L}{c}\left(\frac{E_{\bar{p}} - E_{\pi}}{pc}\right) \qquad (2)$$

$$= \tau\left[\sqrt{1+\left(\frac{m_{\bar{p}}c}{p}\right)^2} - \sqrt{1+\left(\frac{m_{\pi}c}{p}\right)^2}\right]\left\{\tau = \frac{L}{c}\right\}$$

and the inverse of this is

$$\frac{a^2c^2}{p^2} = \frac{\Delta}{\tau}\left[\frac{\Delta}{\tau}\,\frac{b^2}{a^2} + 2\sqrt{1+\left(\frac{\Delta}{\tau}\right)^2\left(\frac{m_{\bar{p}}m_{\pi}}{a^2}\right)^2}\right] \qquad (3)$$

$$\left\{a^2 = \left(m_{\bar{p}}^2 - m_{\pi}^2\right) > 0,\ b^2 = \left(m_{\bar{p}}^2 + m_{\pi}^2\right),\ \tau = \frac{L}{c}\right\}$$

Fainberg and Kalogeropoulos[1] show that the AGS bunch may be adjusted so that, including the resolving time of their detecting circuit, the proton density falls off as $e^{\frac{-t}{\tau_B}}$, where τ_B = 3.7 nsec, on either side of bunch center. Using their detector as a practical example, and taking the position that we want the overlapping π^- intensity to be down by a factor of $r = 10^3$, we would set

$$\delta = \tau_B\,(\ell nr) = 25.6 \text{ n sec.} \qquad (4)$$

in Equation (1).

To the extent that the pion decay helps to purify the beam, the overlap bands would tend to become narrower with increasing decay length L. If one could effectively remove the resultant muons at the end of the beam, then in such an ideal case the overlap band widths would taper to zero, and remain so, where

$$e^{-\frac{L}{c\tau_{\pi}}\,\frac{m_{\pi}c}{p}} \leqslant \frac{1}{r} \quad \left\{\tau_{\pi} = \text{pion lifetime}\right\}$$

Equation (4) would be replaced by

$$\delta = \tau_B \left[\ell n\ r - \frac{L}{c\tau_\pi} \quad \frac{m_\pi c}{p} \right] \gtrless 0 \qquad (5)$$

Substituting this in Equation (1), the overlap bands may be calculated from (2) or (3). They are shown in Fig. 1. Without the pion decay, each overlap band would have an approximately uniform width on the log-log plot.

III. The Long Transport Section

Since Fig. 1 indicates that a TSB will be hundreds of meters in length, an economical optical system must be designed to transport a large phase space over a long distance. Given the 28 eight inch aperture quadrupoles that we will obtain from SREL, this is not a difficult problem, in principal, since a simple alternating gradient channel (AGC) can accept a relatively large transverse phase space over a substantial momentum band, say $\pm$ 10% or more. A plot of the betatron oscillation function β_{max} (at the center of a focussing quad) versus quadrupole focal strength exhibits a very broad minimum; i.e., the acceptance $E = \pi \frac{a^2}{\beta_{max}}$ varies slowly over a wide range of momenta. This behaviour is illustrated in Fig. 2, which is drawn for the case of thin lenses (a good approximation for the channels of interest here). We see that if the quads are spaced by a distance ℓ on centers, $\beta_{max}/\ell \doteq 3.35$. Hence, the acceptance in the initially focussing plane is

$$E_f = \pi \frac{a^2}{3.35\ell}$$

where a = quad aperture radius.

In the other plane, there is more variation in the aspect ratios of the (upright) admittance ellipses, but nevertheless, over $\pm$ 10% in momentum, the common area accepted is still about 90% of E_f.

The total transverse acceptance of the AGC is then

$$E_f E_d \doteq (.9) \left(\frac{\pi}{3.35}\right)^2 \frac{a^4}{\ell^2}$$

If the source has semi-widths of w_x and w_y and emits into semi-angles $\Delta x'$ and $\Delta x'$, then equating source emittance to channel admittance, we have

$$(\pi w_x \Delta x')(\pi w_y \Delta y') = E_f E_d \doteq (.9)\frac{\pi^2}{(3.35)^2}\left(\frac{a^2}{\ell}\right)^2$$

The accepted solid angle is therefore:

$$\Delta\Omega = \pi \Delta x' \Delta y' \doteq \frac{.9\pi}{(3.35)^2}\left(\frac{a^2}{w_x w_y}\right)\left(\frac{a}{\ell}\right)^2 \qquad (7)$$

As an example, suppose we distribute the 30 quads over 300 meters, then $\ell \doteq$ 400" while a = 3.75". A typical AGS target corresponds to $w_x\, w_y$ = 0.1" x 0.05". This leads to $\Delta\Omega$ = 62 mster which, multiplied by a momentum band of $\pm$ 10% or so, would mean a very substantial acceptance. The catch is encountered in trying to perform the emittance match implicit in Eq.(7) over a wide momentum range; the actual acceptance realized is much smaller. This problem will be discussed further in Section V.

As pointed out by Kalogeropoulos, the TSB momentum range need not be restricted to the range between the n = 0 and n = 1 boundaries of Fig. 1. The n = 1 and n = 2 overlap bands are separated by about $\Delta p/p = \pm$ 15%, while $\Delta p/p = \pm$ 9% is the n = 2 to n = 3 separation. Thus, if the transport system is arranged to select momentum bites less than these amounts, the beam may be used at momenta below the n = 1 overlap band.

IV. Momentum Selection

A unit cell with a phase shift of $\pi/2$ lies near the broad minimum in β_{max}. Selecting this phase shift for the AGC allows one to neatly embed two equal bend dipoles early in the lattice, separated by $\Delta\Psi = \pi$, with a Δp defining slit at $\Delta\Psi \doteq \pi/2$. The remainder of the channel is then approximately adispersive. The momentum recombination is not exact, of course, due to the chromatic aberration in the quads. The effect of the residual dispersion was observed in the particle loss pattern, downstream of the dipoles, in the Monte Carlo calculations of Section VII.

A bend in the beam line is also imperative to prevent an intense proton beam from entering the AGC. The proton separation can also be aided by employing a non-zero (0.5°-1.0°) $\bar{p}$ production angle. After the proton beam separates from the negative TSB, it can be dumped in a beam stop or, at some expense, deflected out to another target location.

In section II, it was remarked that pion decay could help to purify the beam if the resulting muons could be removed. This could be largely accomplished by means of another momentum defining section, at the end of the AGC, similar to the one just described. Such a section has not been included in the examples below because it is quite likely that some users will wish to have an even higher resolution arrangement for the purpose of measuring individual incoming particle momenta. The details of such a beam spectrometer will be experiment dependent and have not been studied carefully as yet.

V. The Entrance Doublet

In Section III, it was mentioned that it is difficult to effect an exact match over a wide momentum band from a small, large solid angle source into an AGC with large aperture and small angular spread. Monte Carlo beam traces were performed to determine how many $\bar{p}$'s could be captured in the channel's acceptance. An exact matching (at $p = p_o$) arrangement of three or four suitably placed quads (with apertures arbitrarily large) was found to exhibit very severe chromatic aberration. The overall emittance into the acceptance of the quad channel was less than that from a simple doublet focussed for a point to parallel condition in both planes. ($H_{22} = V_{22} = 0$). Consequently, such a doublet was chosen as the basic objective lens for the system.

An attempt was made to correct the chromatic aberration of the objective doublet by inserting sextupoles and additional dipoles in the first 4 cells ($\Delta\Psi = 2\pi$) of the transport channel. This approach was suggested by a method

devised by K. Brown[5] to eliminate the 2nd order chromatic (momentum-dependent) terms in a curved AG lattice. Using the program TRANSPORT,[6] it was possible to make various ($\delta p \delta \xi_T$) terms of the second order transformation matrix go to zero or, alternatively, to minimize the effects of these terms on an ellipsoid representing the $\bar{p}$ emittance. Although the method works very nicely for the chromatic aberration arising in the lattice itself, it did not seem to be effective in reducing the chromatic effect of the objective doublet, which is the dominant source in this case. In fact, all the "solutions" obtained for the sextupole scheme led to lower fluxes, eventually transported through the remainder of the channel, then were obtained with no sextupoles and only two bends for momentum selection-recombination. In addition, a "gentler" match, combining the quads in the first two cells of the AGC with the doublet, was also tried, again with inferior results.

For given maximum pole tip fields and apertures, the optimum doublet configuration depends on momentum, with longer quads required for higher momenta. In an attempt to approximate the optimum doublet over a range of momenta, the front ends of the example beams described here have four quadrupoles at the front end. The scheme then, is to use Q1 and Q2 as the collecting doublet at the lowest momenta, with Q3 and Q4 set to some "neutral" condition. ("Neutral" is hazily defined as some set of fields which tends to minimize spreading of the p beam before it enters the quad channel. This point hasn't been investigated yet, and so, in the example beams described, the fields were set to zero.) For intermediate momenta, the first element of the doublet would be (Q1,Q2) together, with Q3 being the second element and with Q4 off. The highest momenta would require the doublet to be (Q1,Q2,Q3), Q4. This works out fairly well since, for the point to parallel condition, the first element of this doublet must be donsiderably stronger than the second.

VI. Spot Focus at Experiment

The final beam spot is formed simply by adding another doublet at the end of the AGC. Since the beam emittance is largest in the vertical plane, the final doublet element was chosen to be vertically focussing for the example beams discussed in the next section. The same doublet was used for both examples for simplicity. It gives a convenient spot size in both cases. The final beam length and momentum range chosen, and experimental needs, would lead to a closer optimization of this doublet.

VII. Example Beams

In order to illustrate the range of possibilities, two AGC examples have been chosen, one with quads spaced 400" on centers and one with them 1200" on centers. Table I lists some pertinent data for the two examples. A conception of the layout of the shorter beam is shown in Fig. 3.

The fourth objective lens, Q4, is horizontally focussing and incorporates the function of the first half quad (½QH1) of the AGC. Similarly, the last AGC quad (½QH16) is included in the 8Q32 which also forms Q5 of the spot focussing doublet. The AGC quads QV1, QH2, and QV2 have 12" apertures to allow for the momentum dispersion in those two cells. Consequently, the 15 cells of the AGC utilize just 26 distinct quads of the 8Q16 or 8Q24 varieties and 3 of the 12Q30 or 12Q40 varieties.

The acceptances ($\Delta\Omega\Delta p/p$) for these two examples, derived from Monte Carlo ray tracing, are illustrated in Figures 4 and 5. In each figure, the continuous curve for the "Optimum Doublet" is derived using two quads operating at maximum pole tip field (assumed to be 3.6 kG/inch x 4.0 inch = 14.4 kG) whose lengths are set differently at each momentum to produce the point to parallel condition desired. The real, fixed length quads employed as described in Section V, produce the stepped acceptances shown. Naturally, on each step, the gradients increase proportionally with p until the maximum

(3.6 kG/inch) is reached, at which point one must step down and use the next longer quad combination. Corresponding $\bar{p}$ yields, calculated from the Sanford-Wang production formula,[7] are shown in Fig. 6. The formula is not reliable below $\sim$ 2.0 GeV/c.

VIII. Alignment and Other Constraints

One must be careful in positioning the quadrupoles in a long alternating gradient channel. For the limited number of cells chosen, 15, the tolerances are stringent but not overly severe. If all quads are randomly positioned with the same rms error, δ_{rms}, then the rms phase space (x,x' say) displacement of the beam axis at the end of the AGC ($\frac{1}{2}$QH16) is on a very nearly upright ellipse with amplitudes

$$\delta x_{rms} = 14.7\ \delta_{rms}$$
$$\delta x'_{rms} = 4.31\ \left(\delta_{rms}/\ell\right)$$

where ℓ is the center to center quad spacing.

If all quads are misaligned in the appropriate phase by an amount $\pm\ \delta$, then the maximum beam displacements at the end of the AGC are:

$$\begin{pmatrix} \delta x_{max} \\ \delta x' \end{pmatrix} = \begin{pmatrix} 59.8\ \delta \\ 11.7\ \delta/\ell \end{pmatrix} \quad \{\text{for max } \delta x\}$$

or

$$\begin{pmatrix} \delta x \cdot \\ \delta x'_{max} \end{pmatrix} = \begin{pmatrix} 40.0\ \delta \\ 17.5\ \delta/\ell \end{pmatrix} \quad \{\text{for max } \delta x'\}$$

The vertical effects at the center of the last vertically focussing quad would be slightly smaller.

Hence, if δ_{rms} = 0.02", the rms displacement near the end of the AGC would be about 0.3" or 8% of the aperture and we would begin to notice a loss of flux. An unfortunate in-phase error of $\pm$ 0.02" could lead to a 1.2" excursion.

Finally, one should note that, from the presently envisaged "D" target position, it is 490 meters to the ISABELLE ring. The long example beam, 924 m, would have to include a vertical rise of perhaps 2 meters in order to be able to pass the TSB beam pipe over the ISABELLE ring tunnel. The AGC quad spacing would have to be tailored to span the cross-over point. Beyond that, to the north, one would have to cope with the recharge basin. There would undoubtedly be a number of other problems. The longest TSB, allowing for an experimental area and muon stop, that could be installed without serious interaction with ISABELLE would be about 450 meters long. Any TSB over $\sim$ 200 m in length will have to make a cut up to $\sim$ 18 feet deep in the hill lying between 5th Avenue and the ISA. It may be preferable to translate the TSB elevation. For instance, two 2° pitching magnets could provide a 10 foot rise over 4 unit cells ($\Delta\psi = 2\pi$), leaving the beam dispersion-free thereafter. There would be some beam loss between the pitchers, but this could be minimized by placing them near horizontally focussing quads.

References

1. A. Fainberg and T. Kalogeropoulos, "The AGS Beam Structure", Accelerator Dept. Informal Report BNL-18938, May 6, 1974.
2. M.Q. Barton, "Some Comments on AGS Bunch Areas", Accelerator Dept. Informal Report, BNL-19076, July 17, 1974.
3. T. Brando, A. Fainberg, T. E. Kalogeropoulos, D. N. Michael, G. S. Tzanakos, "Observation of Low Energy Anti-neutrons in a Time Separated Neutral Beam at the AGS", Dept. of Physics, Syracuse University (to be published).
4. Private Communication and Letter of Intent.
5. Private Communication.
6. K.L. Brown, F. Rothacker, D.C. Carey, Ch. Iselin, "Transport - A Computer Program for Designing Charged Particle Beam Transport Systems", SLAC-91, Rev. 2, May 1977.
7. J. R. Sanford and C. L. Wang, "Empirical Formulas for Particle Production in P-Be Collisions Between 10 and 35 GeV/c", Accelerator Department AGS Internal Report JRS/CLW-2, May 1, 1967.

TABLE I: EXAMPLE BEAMS

Overall Length:	314 m	924 m
Objective Lenses:	3 ea-8Q24	3 ea-8Q32
	1 ea-8Q32	1 ea-8Q48
AGC Lattice:	15 cells	15 cells
	400" on Centers	1200" on Centers
AGC Quads:	26 ea-8Q26 (or 8Q24)	26 ea-8Q16(24)
	3 ea-12Q30 (or 12Q40)	3 ea-12Q30(40)
Dipole Bends:	2 ea-18D36, 2° each	2 ea-18D36, 2/3° each
Spot Focus:	1 ea-8Q32	1 ea-8Q32
	1 ea-8Q48	1 ea-8Q48
Spot: RMS Widths	.44"H x .17" V	.18"H x .08"V
Base Widths	2.4"H x 0.8"V	1.2"H x 0.7"V
Separable p	$\sim$ 1.5 - 4.2 GeV/c	$\sim$ 2.7 - 7.8 GeV/c
	$\sim$ 1.0 - 1.1 GeV/c	$\sim$ 1.8 - 2.15 GeV/c
	$\sim$ 0.8 GeV/c	$\sim$ 1.47 GeV/c
Acceptances: $\Delta\Omega\Delta p/p$	1.47 msr	0.35 msr
	0.72 msr	0.26 msr
	0.42 msr	0.16 msr

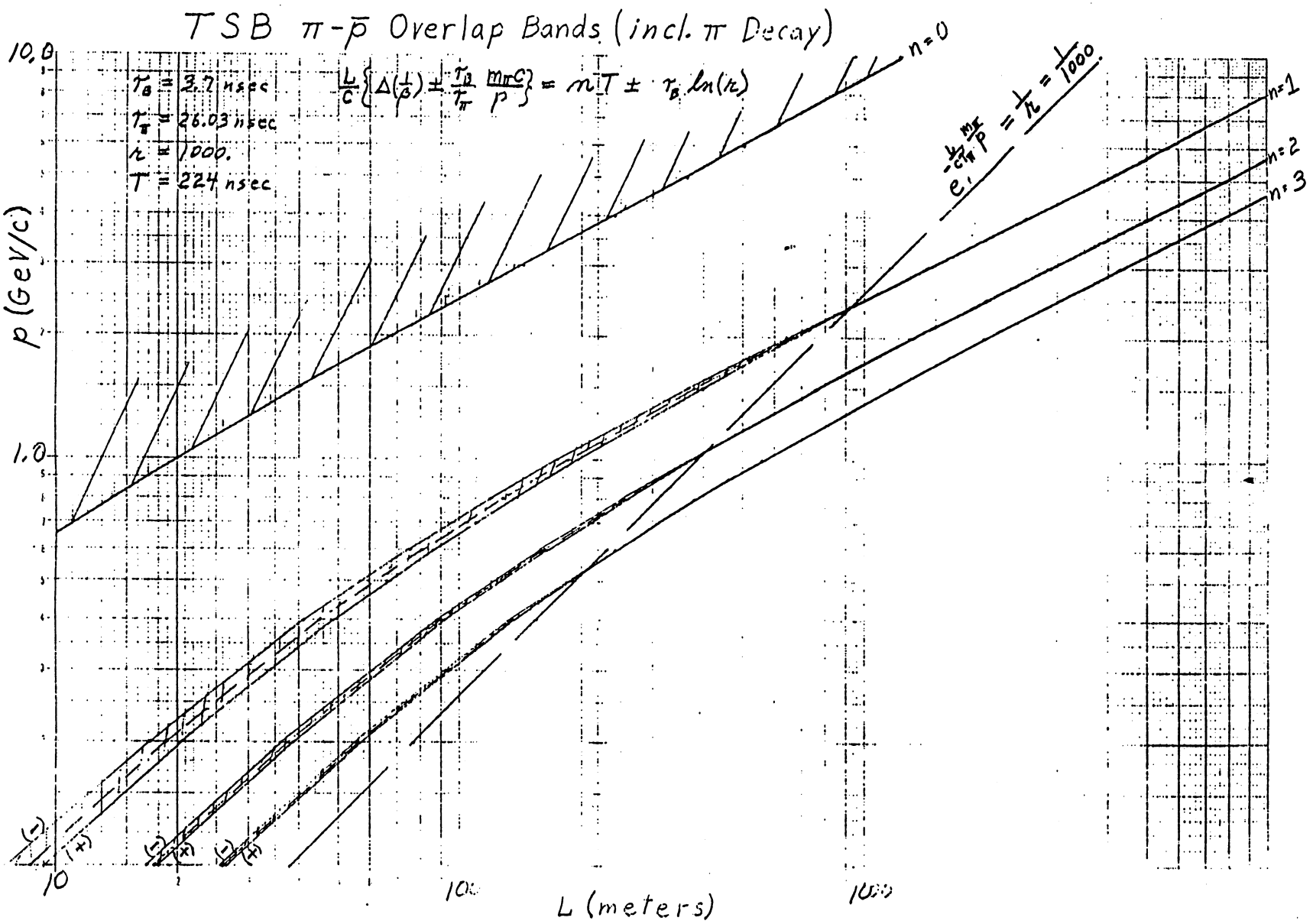

Fig. 1. $\bar{p}$-π Overlap Bands

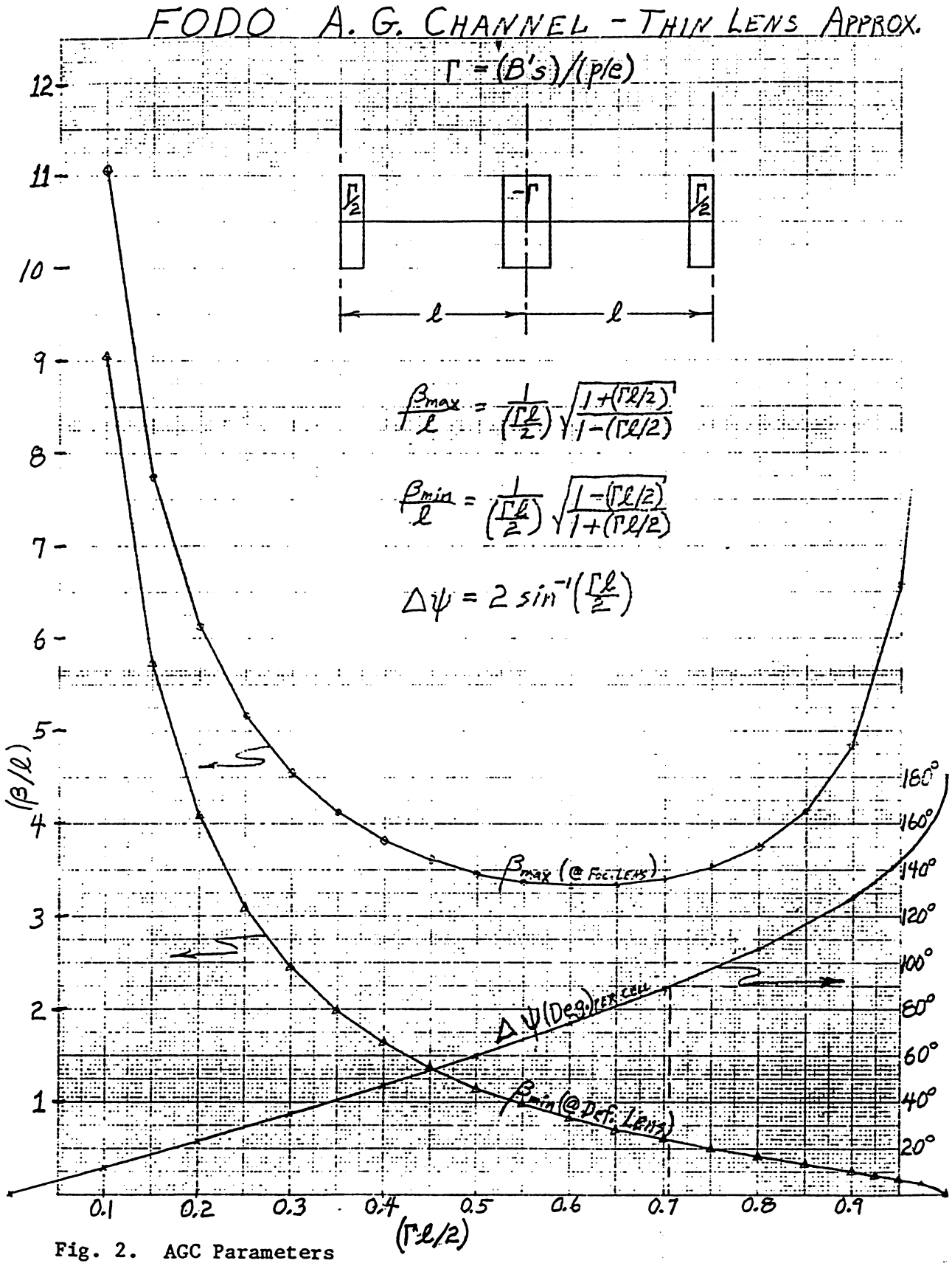

Fig. 2. AGC Parameters

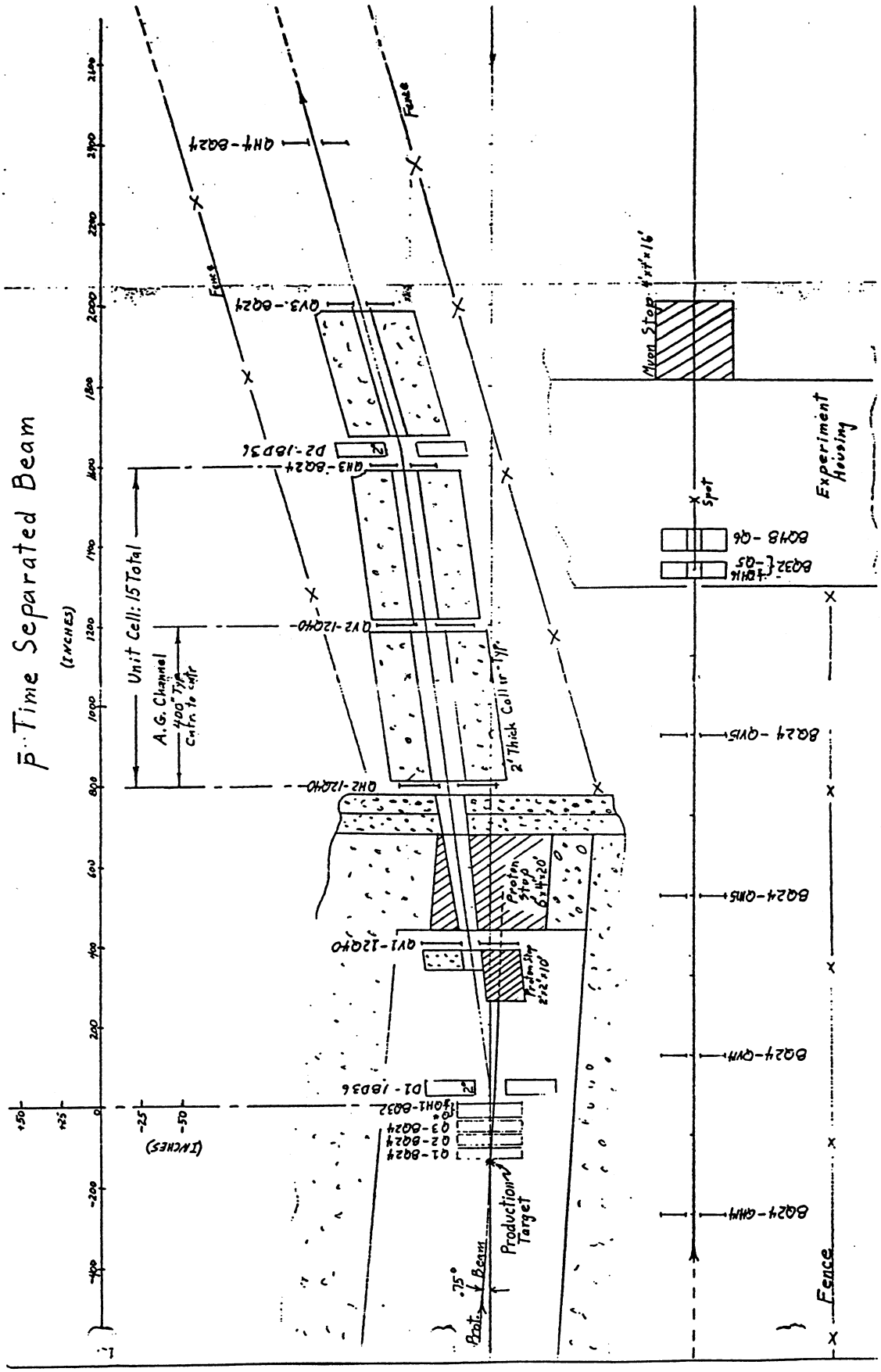

Fig. 3. Plan Drawing of 314 m TSB

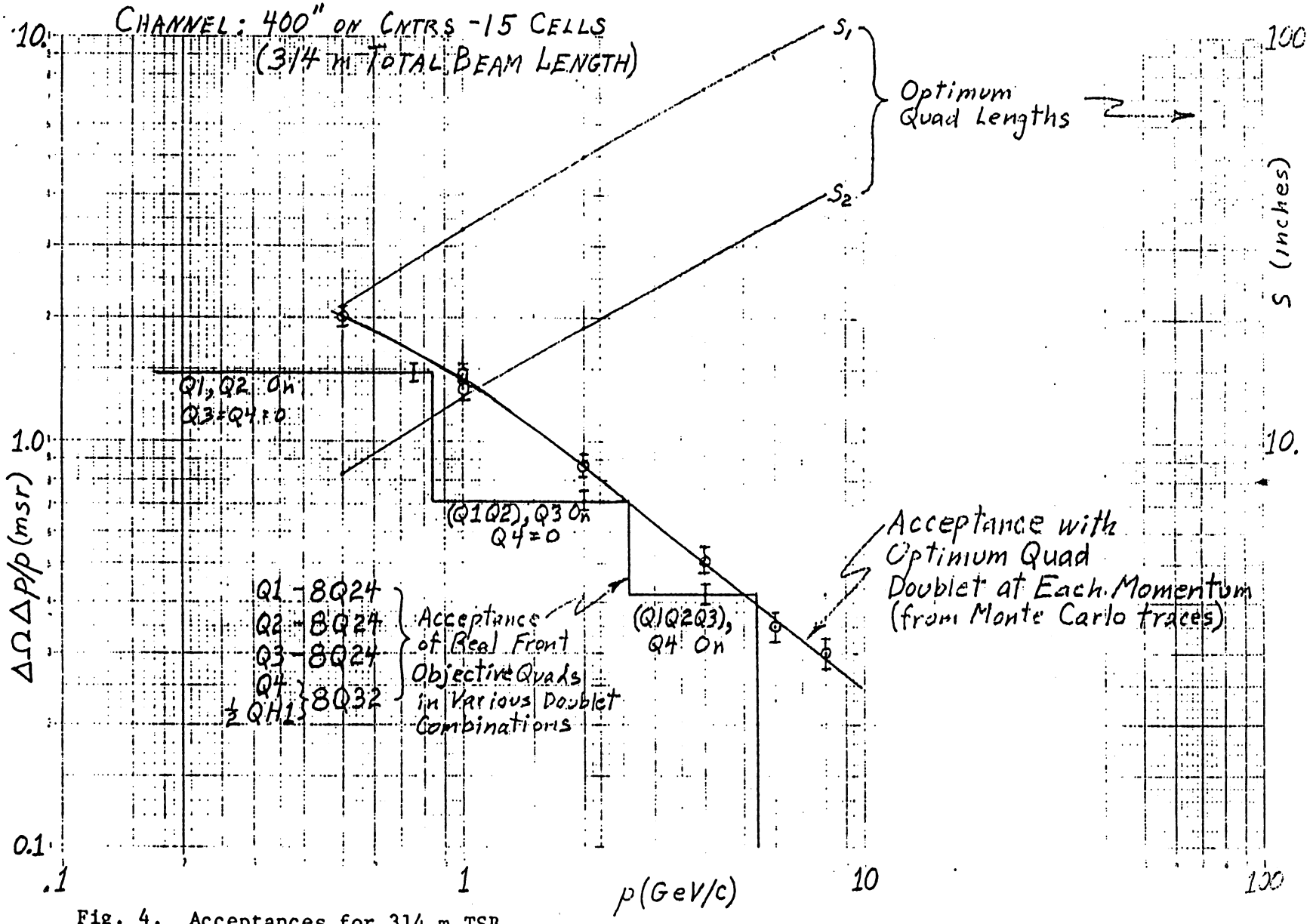

Fig. 4. Acceptances for 314 m TSB

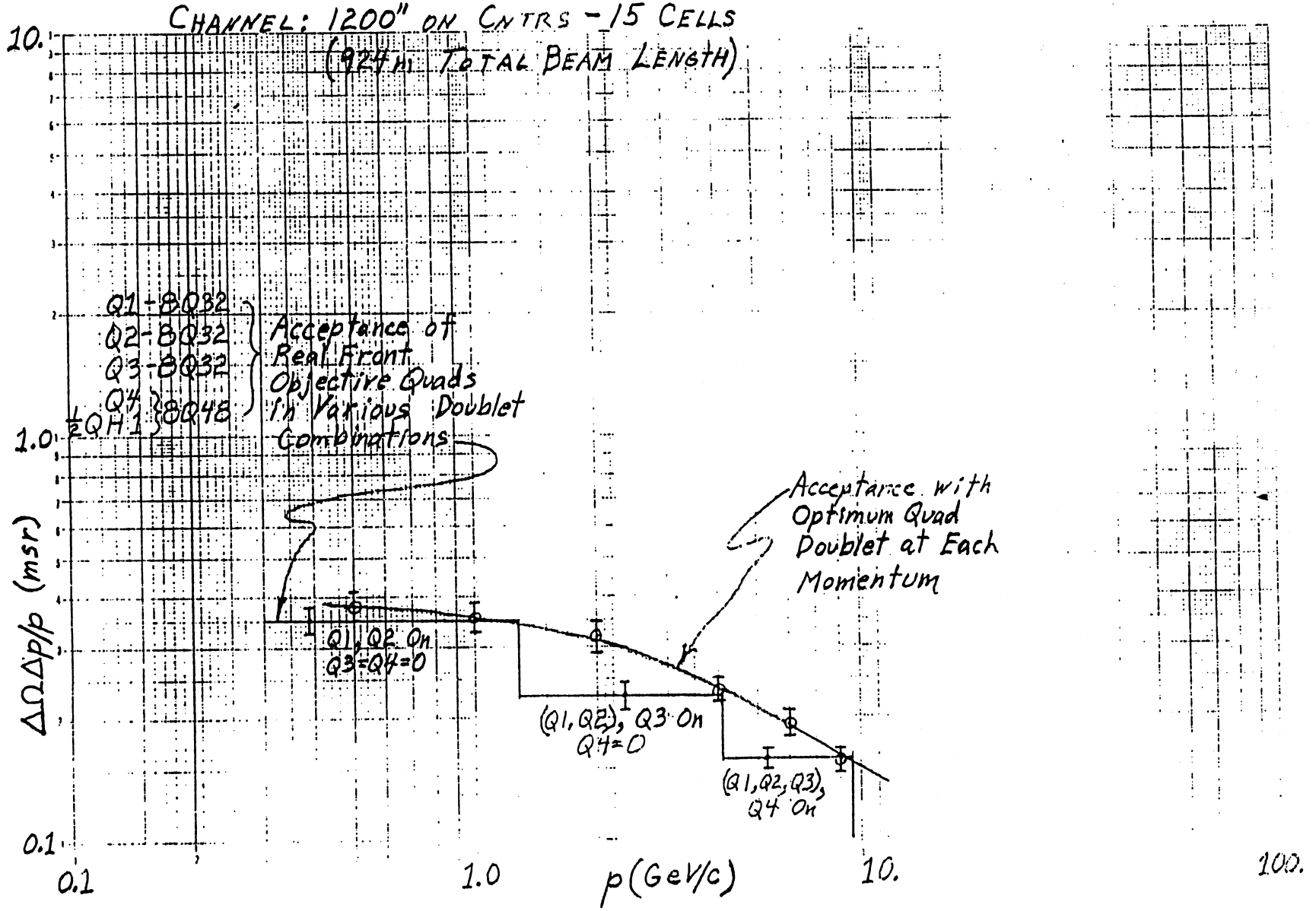

Fig. 5. Acceptances of 924 m TSB

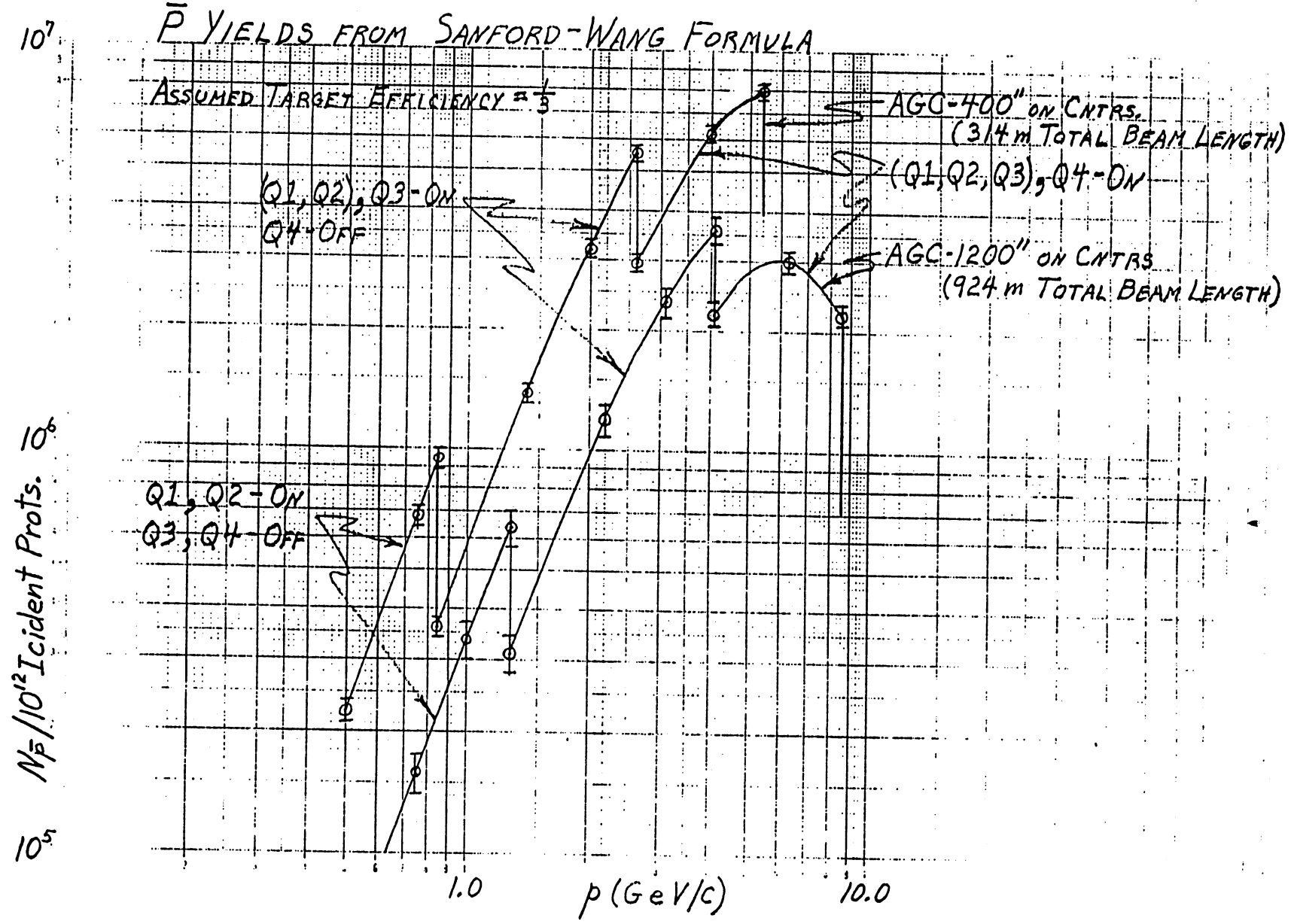

Fig. 6. Calculated Anti-Proton Yields

APPENDIX 3. General Remarks on Antiproton Beams

H. Poth

I. Beam Momentum Spread vs CMS Resolution

The momentum resolution ($\Delta p/p$) of the $\bar{p}$ beam incident on a hydrogen target is related to the center-of-mass resolution by

$$\Delta s^{1/2}/s^{1/2} = 0.5 \times (1 - 1/\gamma) \times \Delta p/p \qquad \text{(A3.1)}$$

where $s^{1/2}$ is the center-of-mass energy. A beam resolution of 0.1% at 5.2 GeV/c ($\gamma = 5.63$) gives, for instance, a mass resolution of 0.04%, which corresponds to 1.4 MeV at the χ_0 mass. $s^{1/2}$ is plotted as a function of $\bar{p}$ momentum for $\frac{\Delta p}{p} = 10^{-4} - 10^{-2}$ in Fig. A3-1.

II. Beam Momentum Resolution

The momentum resolution of each beam is determined by its longitudinal acceptance (momentum bite) unless a momentum analysis is done. This can be performed in two ways:

1. Time-of-flight (TOF) measurements.
2. Beam spectrometry.

The momentum resolution achievable through a TOF measurement is

$$\frac{\Delta p}{p} = 0.3\ \beta\gamma^2\ \frac{\Delta t}{L} = 0.3\ \left(\frac{p}{m}\right)\left[1 + \left(\frac{p}{m}\right)^2\right]^{1/2}\ \frac{\Delta t}{L} \qquad \text{(A3.2)}$$

where Δt is the time-of-flight resolution of the counter system in ns and L is the flight path in meters. For a beam of 0.8 km length and fast detectors with $\Delta t = 0.1$ ns, the momentum resolution at 2.5 GeV/c ($\gamma = 2.85$) becomes $\Delta p/p = 3 \times 10^{-4}$, which corresponds to a cms resolution of the order of 250 KeV but at 5 GeV/c it would only be 1.4 MeV resulting from a momentum resolution of 10^{-3}.

High energy spectrometers achieve typical resolving powers of 10^{-4} or better at a momenta below 1 GeV/c. It might be possible to obtain similar values with a beam spectrometer by having a large dispersion by a suitable bend and a spatial resolution of 1 mm., e.g. a beam of 4% momentum spread dispersed over 40 cm. This ignores its finite emittance whose effect is discussed in Appendix 4.

III. Energy Loss in Target

Minimum ionizing particles lose 4.12 MeV per g/cm^2 in liquid hydrogen. The energy loss ΔT in the target can be related to cms resolution $\Delta s^{1/2}$ by

$$\Delta s^{1/2}\,(\text{MeV}) = m\, s^{-1/2}\,(\Delta T) = 938 \times s^{-1/2} \times (4.12 \times 0.0709\ d)$$
$$= 274\ d(\text{cm})/s^{1/2}(\text{MeV}) \qquad \text{(A3.3)}$$

where m is the mass of proton or antiproton and d is the target length. Thus, a mass resolution of 1 MeV at the χ_0 mass of $s^{1/2} = 3415$ MeV corresponds to 12.5 cm of liquid hydrogen of density 0.0709 g/cm^3.

From the above considerations it is concluded that experiments aiming at a mass resolution of 1 MeV in the range under discussion should be possible with a beam momentum analysis of 10^{-3} and vertex reconstruction to a few centimeters.

IV. Beam Purity

If no particular measures are taken, the purity of the $\bar{p}$ beam depends entirely on the length of the beam and its bends. The number of pions remaining after a given flight path L can be approximated by

$$N_\pi\,(L) \approx N_\pi\,(0)\ \exp\,(-17.9\ L/p) \qquad \text{(A3.4)}$$

Here L is to be taken in km and the beam momentum p in GeV/c. A beam of 0.8 km length therefore as a $\bar{p}$ purification factor (pion rejection factor) of 60 at 3.5 GeV/c but only 4 at 10 GeV/c. Figure A3-2 gives the ratio of Eq. (A3.4) to $\bar{p}$ flux for beam lengths of interest. Without a highly dispersive bend such as the high resoution beam spectrometer, beam counters will still be subject to high muon rates.

V. Achievable Luminosity

The luminosity with an external beam and an external target can be calculated:

$$L = F\ R\ \rho\ d\ N_o/A \qquad \text{(A3.5)}$$

where F is the flux of $\bar{p}$ per incident proton, R is the flux of incident protons, ρ is the density of the $\bar{p}$ target, N is Avogardro's number, A the atomic weight of the target material and d the target length. A 56 cm long target of liquid hydrogen has an area density of about 4 g/cm^2. Upon insertion of F from Eq. (1.2) and assumption of $R = 10^{12}$/sec at the present AGS, the achievable luminosity at the $\bar{p}$ production maximum becomes $L = 5 \times 10^{30}$ $(cm^2\ sec)^{-1}$. The total $\bar{p}p$ cross section at 5-6 GeV/c is about 60 mb: hence a reaction rate of about 300,000 per second in the target, out of which one must filter a specific reaction of interest (e.g., charmonium production).

The above luminosity is comparable to what is anticipated for E760 at Fermilab. The present luminosity will be lower at other momenta, however, due to falloff in the $\bar{p}$ production rate.

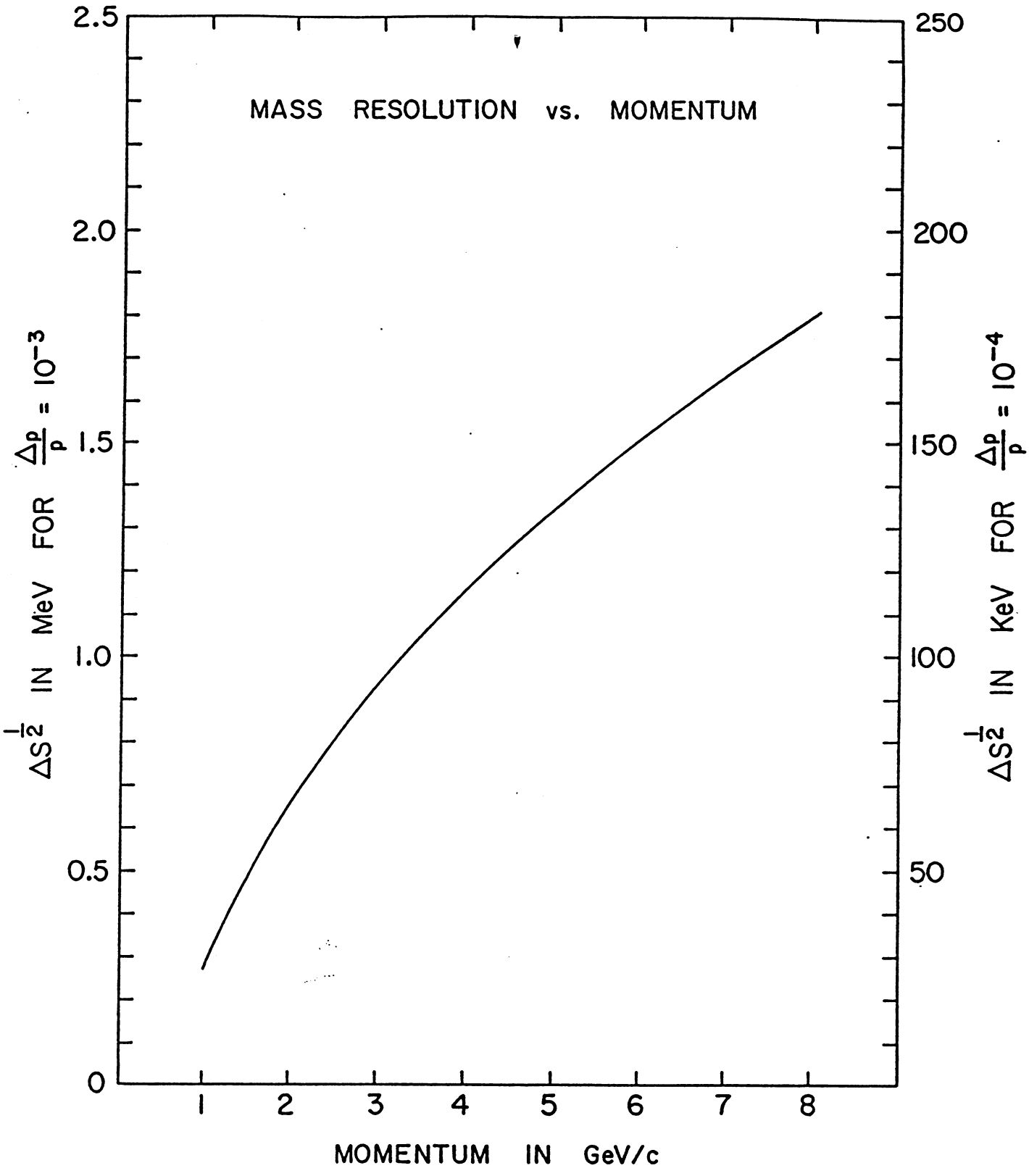

Fig. A3-1. cms Mass Resolution vs. $\bar{p}$ Momentum

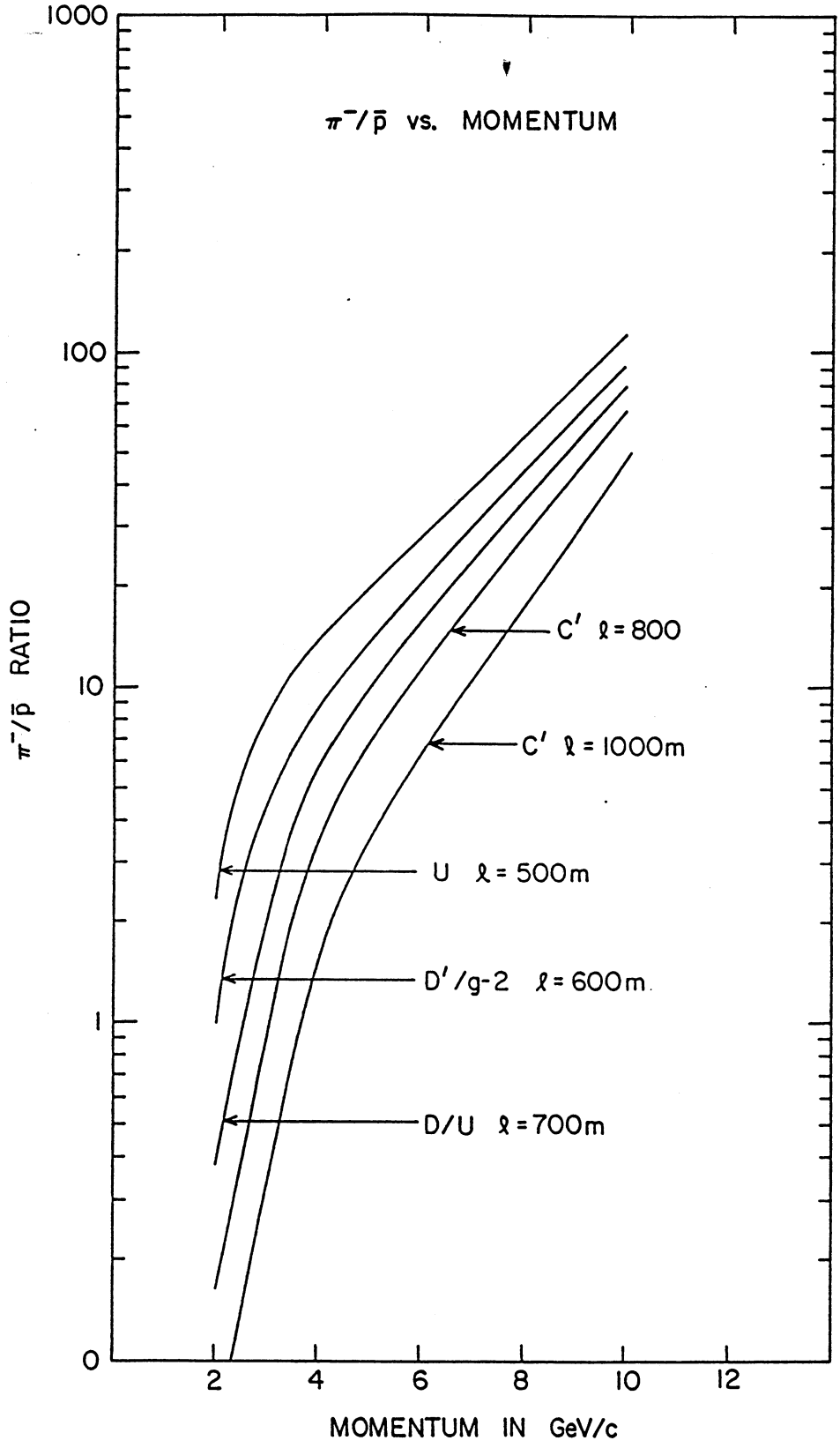

Fig. A3-2. Purity of Various $\bar{p}$ Beams

APPENDIX 4. Beam Momentum Resolution

J.W. Glenn, III

The momentum resolution of a beam obviously depends on the analyzing bend angle and less obviously on the emittance of the beam and the size of the focusing elements before the momentum defining elements, since it depends on the spot size as well as the dispersion.

Assume a system that has the analyzing bend at the focusing elements which create the spot at the momentum defining elements (more complex systems can be approximated by this). The resolution R (where larger R implies poorer resolution) is defined as:

$$R = \frac{X}{\frac{dX}{\Delta p/p}} \tag{A4.1}$$

where X is the beam half-size and the dispersion $\frac{dX}{dp/p}$ is the change in beam position per fractional change in momentum. But

$$\frac{dX}{\Delta p/p} = L\alpha \tag{A4.2}$$

where L is the length of drift after a bend of α radians. The minimum size obtainable after drift L is

$$X = L\varepsilon/Y \tag{A4.3}$$

where ε is the emittance of the beam and Y the beam half-size at the start of the drift (limited by quadrupole aperture). Thus,

$$R = \frac{L\ \varepsilon/Y}{L\ \alpha} = \frac{\varepsilon}{\alpha\ Y} \tag{A4.4}$$

The length drops out: a large drift implying a large spot, also a large dispersion.

In the decay purified antiproton beam leading into the RHIC injection area, a 7.5° vertical bend with a 12Q30 and 6RQ24 vertically focused doublet has been suggested. The vertical aperture of 24" in the 6RQ24 combined with an emittance of 6 mm-mrad gives a resolution of 1.5×10^{-4}. Any degradation in emittance--e.g., gas and window scattering

after the emittance defining elements--degrades the resolution, as will any spot size increase due to field errors in the focusing elements.

It should be noted that the emittance of the beam is proportional to the production target size, i.e. the proton beam spot, and the angles accepted in the secondary beam line. Thus, the larger the target, the poorer the resolution; and the larger the angle accepted, and hence the higher the intensity, the poorer the resolution. To optimize the resolution, the production target should be placed where the smallest proton beam would be available.

APPENDIX 5. High Field Properties of the AGS Booster Dipole Magnet

G. T. Danby and J. W. Jackson

The booster dipole high field properties are of interest in determining the highest energy to be available for various possible booster modes of operation. This in principle can include applications not originally planned for: antiprotons, for example.

1. Original design choices[1]

a. Rapid acceleration for multiple pulse injection (up to 10 Hz) into the AGS for high proton current operation required a magnet design with minimum stored energy consistent with aperture requirements.

b. High intensity proton operation, as well as the function of accumulating many turns of polarized protons, required a large aperture with excellent field properties from injection up to intermediate fields.

c. Heavy ion acceleration required slow acceleration, 1/2 second rise time, up to 12 kG. This has recently been raised to 12.7 kG. The highest field is related to optimum stripping efficiencies of heavy ions in transit from the booster to the AGS.

d. The pole width chosen was the minimum required to give the necessary injection good field aperture, extending essentially over the entire vacuum pipe.

e. The narrow pole with commensurately small cross section yoke return, wrapped around tight fitting coils located above and below the high field region, provides the low stored energy.

f. As 12 kG is approached, sextupole effects begin to grow very slowly, producing only $\Delta B/B_o = 10^{-4}$ at r = 1 inch. This was a design specification.

g. Above 12 kG dipolar saturation commences because of the small iron cross section. Aberrations in the field quality--sextupole, etc.--grow very slowly, however, if the magnet is excited above its maximum design field.

---

[1] Accumulator/Booster Proposal for the AGS, BNL 32949-R, February 1984.

h. Saturation is predominantly sextupolar: Operation of lattice correction sextupoles can to first order cancel the effect of this aberration for larger apertures if desired, or for higher field operation.

2. Possible use of the booster as an antiproton storage ring

a. Antiprotons produced at an AGS target station at the optimum production energy could be injected into the booster.

b. They could be stored, or accelerated/decelerated prior to storage.

c. As an alternative to acceleration, production could occur at non-optimum production energy, and storage carried out without acceleration.

d. Strong interest was expressed in the possible operation of the booster as a storage ring up to 6.5 GeV/c, i.e., 25% higher energy than its design value. This is in order to reach interesting $\bar{p}p$ resonances. This is clearly the hardest question.

3. Discussion of low energy $\bar{p}$ possibilities

a. The excellent low field properties of the booster magnets is very helpful to low field storage possibilities.

b. Antiprotons might be decelerated to low energies and transferred to a small ring or "bottle."

c. The large number of free straight sections available might accommodate cooling apparatus at low energies where cooling is most efficient.

d. A cooled beam might then be accelerated to higher energies with higher beam intensity.

Comment: The above possibilities seem to be permitted from a magnetic point of view. Quantities of low frequency rf, beam cooling, etc., are at this point just speculation but appear worth pursuing.

4. Discussion of high energy $\bar{p}$ possibilities

We now turn to the high field computer dipole magnet study, which is the "meat" of this report.

Figure A5-1 shows the field deviation $\Delta B/B_o$ on the horizontal midplane (HMP). Note that these results were computed for 100% steel packing factor and for a decarburized iron permeability table. If the packing factor was 95%, for example, the saturation aberration shown would occur at 5% lower central field than computed. This is illustrated in brackets in Fig. A5-1.

Table A5-1 lists the multipole content of the field as a function of dipole field. The multipoles are expressed as parts in 10^4 of the dipole at a radius of 1.5 inches. The signs correspond to the coordinates (r,y = +1.5 in., 0 in.). Note that the multipoles are also tabulated for 100% packing factor. For a packing factor of 95%, for example, the multipoles listed at 15 kG will occur at 15 x 95% = 14.25 kG. It can be seen that for 15 kG operation, assuming the lattice sextupoles roughly compensate for the b_2 saturation, the residual 10-pole aberration is $\sim 3 \times 10^{-4}$ $\Delta B/B_o$ at r = 1.5 in. This corresponds to a roughly circular good field region.

In summary, from an acceptable field aberration point of view, the magnets can be powered significantly above the design field of 12.7 kG. Their actual performance will depend on the steel properties: chemistry (permeability), thickness of laminations, thickness of insulating layer and compression of laminations. These will soon be much better known for the actual production magnet steel.

As far as aberrations are concerned, silicon steel should behave as well as decarburized iron, since it normally outperforms soft iron below 16 kG. As a result, a small packing factor correction to the multipoles tabulated from the computer results for 100% packing factor is credible.

The "bad news" is shown in Fig. A5-2, which gives the dipolar saturation. The "ampfac" is the increase in I/B due to finite permeability, plotted versus aperture field B. For example, the increased current at B = 15 kG is 18% above that which would be required for $\mu = \infty$ and for 100 packing factor. Note that the alternate horizontal scale of B (below the computed scale) which corresponds to 95% packing factor with decarburized iron.

Silicon steel will also effectively displace the curve in a similar manner, since it has inferior permeability properties at very high fields (i.e., in the iron flux returns of the magnet). This dipolar saturation is dominated by the narrow poles and flux returns: saturation being designed to commence at 12 kG.

Table 5-2 lists the currents corresponding to various fields with 100% packing factor and also with 95% packing factor. The 95% values are likely to be reasonably close to the actual I/B magnet performance. This is roughly sufficient to allow for both the actual packing factor and a contribution from the reduced performance of silicon steel.

These computations will be repeated with the final steel laminated magnet properties when available.

5. Is very high field operation practical?

This is not easily answered (note that 6.5 GeV/c requires 15.77 kG).

a. The dipole magnet power required is about 70 KW per unit, or roughly 3 MW for all dipoles.

b. For quite slow cycling or dc operation the power supply required is not excessive.

c. The quadrupoles have not been considered at this time, but if a problem occurred, they could always be operated at a lower tune.

d. Bussing and connections would have to be designed for significantly higher power than originally considered (~ 2x). Water flow capability would have to be suitably increased.

e. Larger fringing fields would occur. This would have to be considered in locating other apparatus that might be field sensitive.

f. In conclusion, more study is required if this option is to be considered seriously.

A policy decision would have to be made to keep high energy $\bar{p}$'s in mind during the booster final design phase. Extra work would be required just to find out whether or not to build in this option. It appears too big a perturbation to try to consider only as an "afterthought."

Table A5-1. BOOSTER DIPOLE FIELD QUALITY

B_o(kG) f=95%	B_o(kG) f=100%	b_2	b_4	b_6	b_8
	1.6	+ 0.04	+0.02	0.00	-0.00
	5.0	- 0.14	+0.02	0.00	-0.00
7.6	8.0	- 0.27	-0.01	-0.00	-0.00
	9.0	- 0.43	-0.07	-0.02	-0.01
9.5	10.0	- 0.71	-0.19	-0.03	-0.01
	11.0	- 1.23	-0.39	-0.09	-0.01
11.4	12.0	- 2.35	-0.81	-0.17	-0.02
	12.5	- 3.30	-1.16	-0.20	-0.02
	13.0	- 4.58	-1.56	-0.22	-0.02
13.3	14.0	- 8.15	-2.37	-0.19	-0.04
	14.5	-10.43	-2.74	-0.17	-0.08
14.25	15.0	-13.03	-3.05	-0.20	-0.09
14.7	15.5	-15.96*	-3.38	-0.27	-0.10

Multipoles expressed in units of 10^{-4} at R = 1.5 inc., Y = 0 in.

* Note that this value corresponds to a sextupole magnet of 6 in. diameter, 4 in. length, and a pole tip field of 2.5 kGauss.

Table A5-2. BOOSTER DIPOLE - CURRENT REQUIREMENTS

B_o (kG)	AMFACC	I_{KA} (KA) f=100%	f=95%
2.4356	1.0	1.000	1.050
5.0	1.0046	2.062	2.165
8.0	1.0054	3.302	3.467
9.0	1.0062	3.718	3.904
10.0	1.0078	4.138	4.345
11.0	1.0019	4.570	4.799
12.0	1.0267	5.058	5.311
13.0	1.0610	5.663	5.946
14.0	1.1116	6.390	6.710
15.0	1.1795	7.264	7.627
15.5	1.2213	7.772	8.161

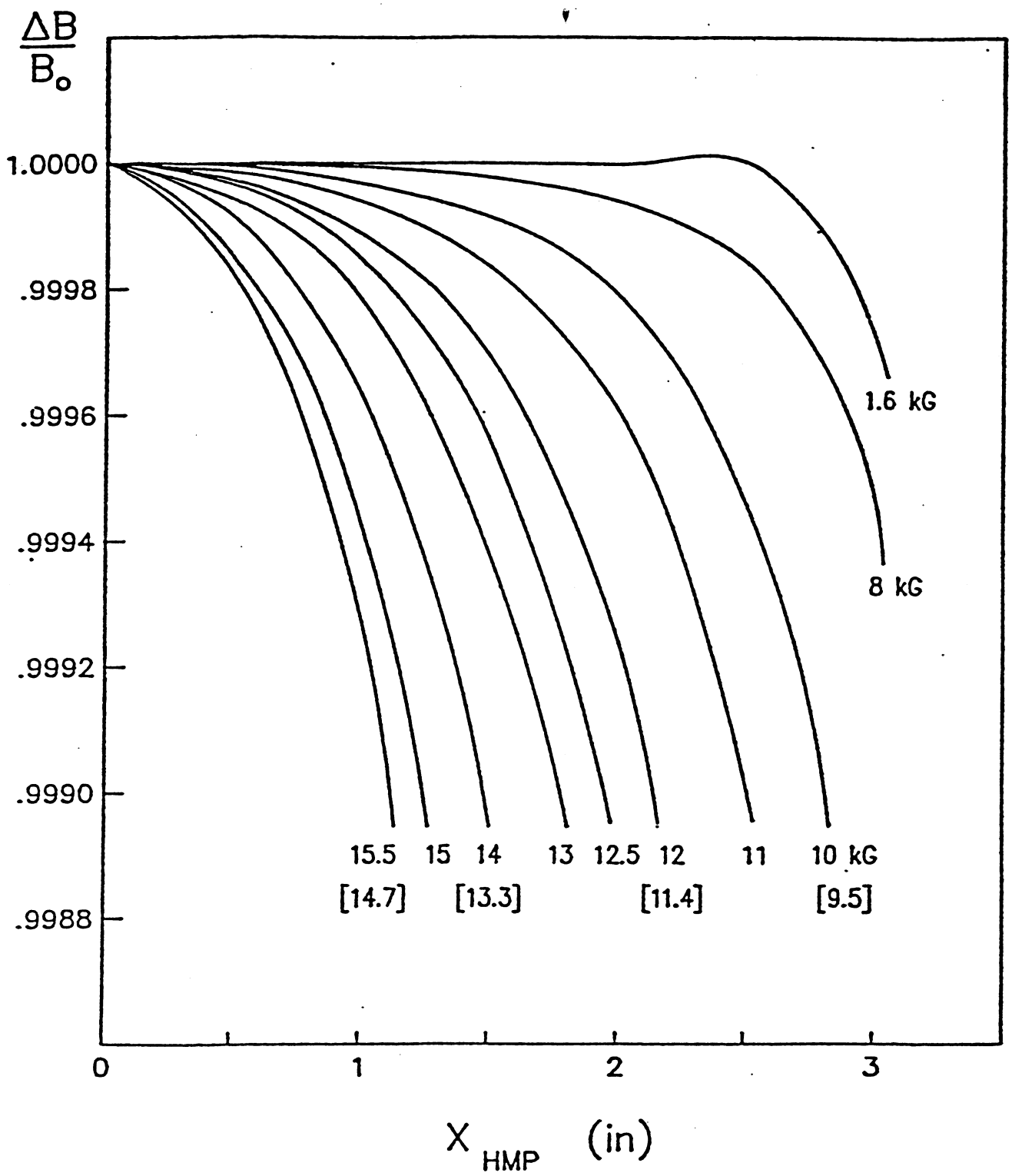

Fig. A5-1. Booster Dipole HMP Field Deviation

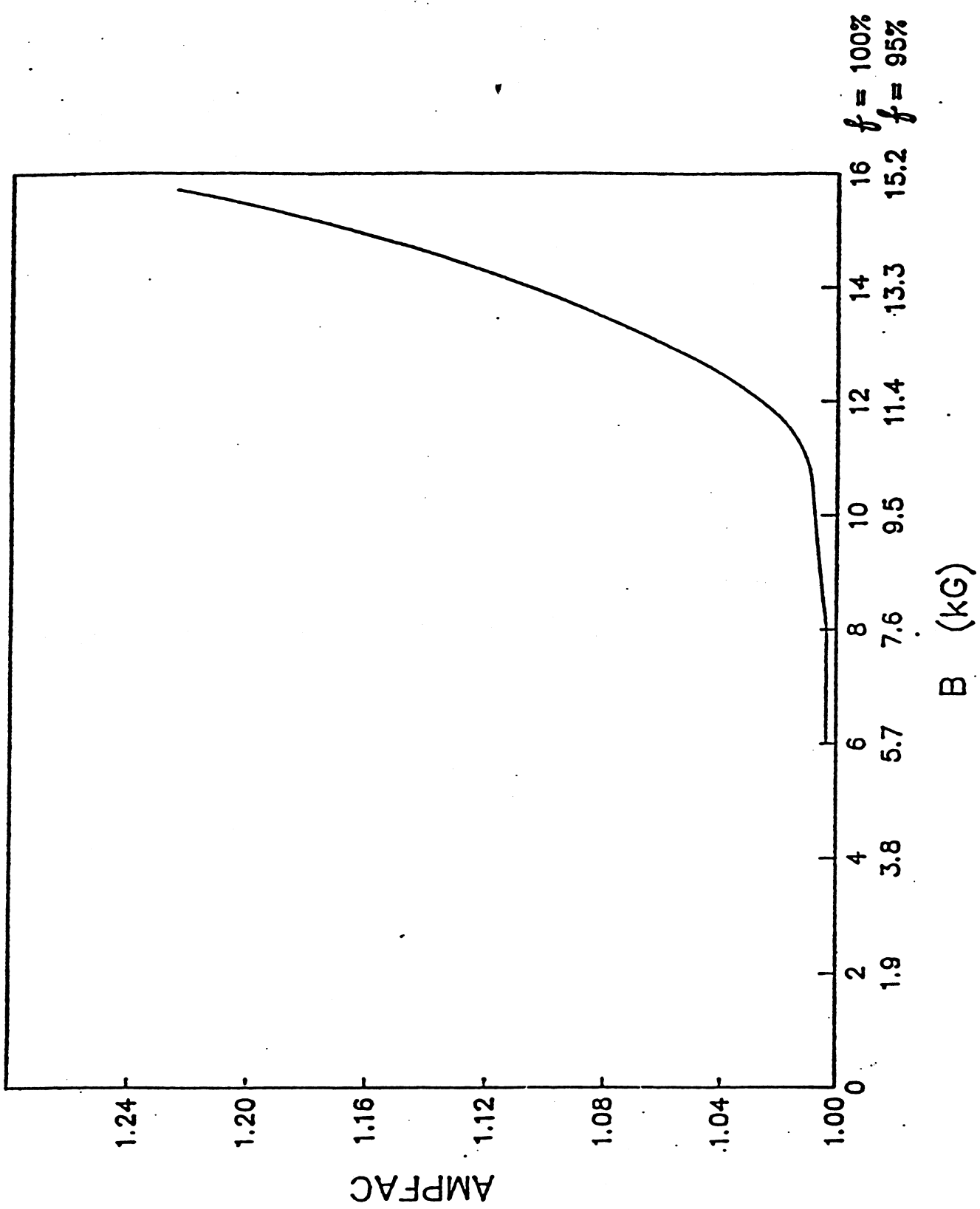

Fig. A5-2. Booster Dipole AMPFAC vs. Central Field

APPENDIX 6. Very Low Energy Antiprotons

Y.Y. Lee

1. Introduction

It has been proposed[1] that the AGS Booster[2] be used as a time stretcher/purifier for antiprotons of momentum .65 to 5.2 GeV/c. The lower limit corresponds to the linac output of 200 MeV kinetic energy. In this note we should like to extend the idea to very low energy antiprotons at tens of KeV kinetic energy.

A brief description of the system has been given in Section 4 of the text. Once the antiprotons are injected and captured in the booster, one can either accelerate or decelerate them. After deceleration to 200 MeV kinetic energy, they can be further decelerated through the linac and an RFQ (radio frequency quadrupole) preinjector down to the ion source energy.

2. Antiprotons without cooling

Assuming the standard yield of antiprotons in Eq. (1.1), $Y = 10^{-6}\ \bar{p}$ (2 mrs % interacting proton)$^{-1}$, one can estimate the number of antiprotons that can be accumulated in the booster acceptance of 50 mm-mr and 2% momentum bite. Realistically the AGS proton beam at 28.4 GeV/c can be focused down to 1 mm spot size, and therefore the angular acceptance one can expect in each dimension would be 50 mm-mr/0.5 mm = 100 mr with the solid angle subtended being 40 msr.

Because of the finite length of the target, the collection efficiency would be reduced further. For a 10 cm long target particle production studies show that only 1/3 of the particles fall into the usable phase space. The corresponding $\bar{p}$ flux is given in Eq. (1.2), which we express as follows:

$$N_{\bar{p}} = 4.0 \times 10^{-6}\ N_p \qquad \text{(A6.1)}$$

where N_p ($N_{\bar{p}}$) is the number of incident protons (usable antiprotons).

The post booster AGS will accelerate .5 x 10^{13} protons/bucket, and if one uses 3 of those buckets for $\bar{p}$ production per cycle,

$$N_{\bar{p}} = 4 \times 10^{-6} \times 1.5 \times 10^{13} \qquad \text{(A6.2)}$$
$$= 6 \times 10^{7}\ \bar{p}/\text{ pulse}$$

at 4 GeV/c, the transport momentum of the antiprotons into the booster.

If one decelerates the collected antiprotons, assuming the rf system has enough debunching to take care of the antiproton beam energy spread, i.e., reduce the energy spread while making the bunch long, then the betatron phase space decreases as $1/p^2$. Deceleration in the booster to momentum p leads to a flux reduction by a factor $(p/4\ \text{GeV/c})^2$. The normalized emittance of the collected beam at 4 GeV/c is 213 mm-mr, and this emittance will be trimmed through the deceleration process. The normalized acceptance of the booster at 200 MeV linac energy is 34.3 mm-mr. Figure A6-1 shows the resultant antiproton intensity as a function of final decelerated kinetic energy in the booster.

3. Deceleration through the linac

The decelerated antiprotons can be extracted near the booster injection channel and transported through either the injection transport system with its dipoles reversed or through a separate transport system to the 200 MeV end of the linac. They are then decelerated to a kinetic energy of 750 GeV at the "entrance" of linac tank 1. The acceptance of the system is dominated by the normalized admittance[3] at the 750 KeV point of 10 mm-mr. Thus, one will lose beam intensity through the 200 MeV linac by a factor of $(10/34.3)^2 = .085$ and by an additional factor of 2 due to beam bunching inefficiency. As a result 0.7 x 10^5 antiprotons will survive to 750 KeV. The antiprotons can be further decelerated through the RFQ preinjector to energies of 20 KeV.

4. Effect of cooling

If one could cool the antiprotons to less than 10 mm-mr normalized o 14.6 mm-mr at 200 MeV energy, theoretically half the 6 x 10^7 antiprotons r collected at 4 GeV/c could be decelerated to 750 KeV and then to 20 KeV.

References

1. A.S. Carroll, Y.Y. Lee, D.C. Peaslee, and L.S. Pinsky, to be published.
2. AGS Booster conceptual design report, BNL 34989R (1985).
3. G.W. Wheeler et al., Particle Accelerators 9, No. 1/2, (1979).

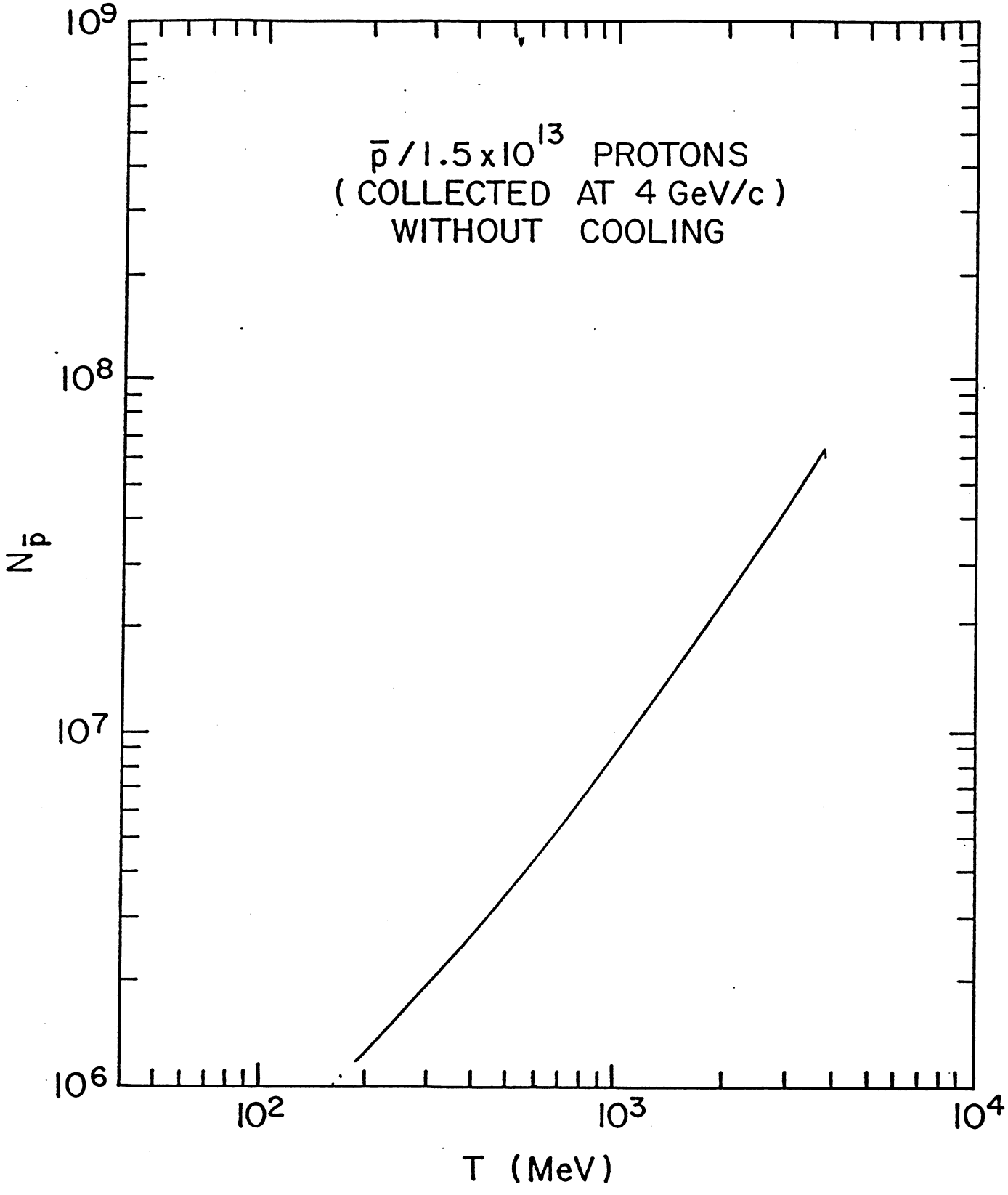

Fig. A6-1. Intensity of Decelerated Antiprotons

APPENDIX 7. Overview of Booster $\bar{p}$ Potential

D.C. Peaslee

I. Introduction

The accompanying studies describe a specific arrangement whereby the proposed AGS Booster can be employed in a parasitic mode to provide an external beam of 2-6 GeV/c antiprotons whenever the AGS operates in the slowly extracted beam mode and is not running polarized protons or heavy ions. This possibility of continuous production, combined with the favorable operating record established by the AGS, can provide an antiproton source unmatched by any other in that momentum range. This conclusion, at first perhaps surprising, is documented below.

II. Continuous parasitic mode: $\bar{p}$ yield

According to Appendix 6 the post-booster AGS will accelerate in every cycle 12 buckets of 0.5×10^{13} protons each, or which 3 are extracted to produce antiprotons while the other 9 buckets are available for the rest of the program. The result is 6×10^{7} $\bar{p}$ pulse, which must be ejected from the booster each cycle of about 2.5 seconds. Typical AGS performance is some 10^{3} pulses/hr for about 10^{2} hr/week when the SEB program is running, a total of around 10^{5} pulses/week. The SEB program of the AGS approaches 20 weeks' running time in a normal year. Thus the potential antiproton yield is of order

$$Y(\text{Booster}) \approx 10^{14}\ \bar{p}/\text{year} \qquad \text{(A7.1)}$$

III. Comparative yield at LEAR

Typical operation at LEAR to-date has consisted[1] of stacking 3×10^{9} antiprotons every 75 minutes, corresponding to 6×10^{10} $\bar{p}$/day. This beam has been provided to experiments[2] about 30 days/yr during the 3 years that LEAR has operated. Thus a $\bar{p}$ yield of

$$Y(\text{LEAR}) = 2 \times 10^{12}\ \bar{p}/\text{year} \qquad \text{(A7.2)}$$

has been available.

A new antiproton source (ACOL) is expected to operate at LEAR in 1987 with an order of magnitude improvement[3] in daily intensity to 10^{12} $\bar{p}$/day, but at no expected increase[2] in duty cycle over 30 days/years; thus,

$$Y(ACOL) = 3 \times 10^{13} \bar{p}/year \qquad (A7.3)$$

It appears that because of its parasitic rather than exclusive operating mode, the expected annual antiproton yield from the Booster is almost 2 orders of magnitude greater than Y(LEAR) and a factor of at least 3 greater than at LEAR after ACOL.

Section 4 of the text indicates that the booster option will be continuously tunable to any desired momenta between about 0.7 and 5.2 GeV/c without modification. There appears to be no technical barrier to increasing that upper limit to around 6.5 GeV/c (Appendix 5); what would be needed is some incremental design study. If we extrapolate to 7 GeV/c, the equivalent of super-LEAR would be available, again with the increase of yield represented by Eq. (A7.1) over (A7.2).

IV. Comparative yield at FINAL: E760

The accumulator at FNAL can be used as an antiproton source in conjunction with an internal gas jet target, as in the recently approved experiment E760. The accumulator is designed[4] to stack 4×10^{11} antiprotons in 4 hours at a momentum of 8.9 GeV/c. During Tevatron collider operation the accumulator will not be available for other purposes. On the other hand, during fixed target running the accumulator could be operated parasitically with perhaps a 50% duty cycle: i.e., stacking about 2×10^{11} antiprotons every 4 hours or some 10^{12} $\bar{p}$/day at 8.9 GeV/c.

Decelerating these antiprotons to arbitrary momenta for experiments with a gas jet target will be difficult because the accumulator was designed as a fixed-energy machine. Losses must be expected; going to the top of the charmonium spectrum at around 7 GeV/c implies a reduction of at least $(7/8.9)^2$ to around 6×10^{11} $\bar{p}$/day. This yield is on the same order as ACOL: if FNAL provides only 30 days/year of antiprotons for the internal target, as at CERN, the effective yield for E760 will be a factor of 3 less than Y(Booster). Of course, there is no previous operating experience at FNAL on which to base estimates, but the importance of high-energy needs vis-a-vis fixed target operation is likely to be no less than at CERN for the forseeable future.

V. Effective luminosity

The effective luminosity of the booster antiproton system may be estimated in a most favorable case as follows: Assume a liquid H_2 target some 2-3 meters long, of order the nuclear mean free path, with detectors arranged along its length to pinpoint the interaction vertex. Then 6 x 10^7 $\bar{p}$/pulse = 2 x 10^7 p/second translates to an effective luminosity

$$L \approx 10^{32}/cm^2 \text{ sec} \qquad (A7.4)$$

This is a full order of magnitude greater than for ACOL or E760, but of course refers to a scan over the 50-100 MeV range of energy loss in the target. While this would be adequate for ordinary hadron resonances, the special narrowness of some charmonium states would impose a reduction on Eq. (A7.4), back to $L' \lesssim 10^{31}/cm^2$ sec. This is comparable to the luminosity expected for E760; there still remains the advantage in expected annual duty cycle of the AGS over FNAL for low energy antiproton operations.

VI. Tunability

The booster cycle described in Section 4 of the text is able to deliver antiprotons at any momentum within its range, even though they are injected at 4 GeV/c. The booster momentum range neatly covers the gap between LEAR ($\lesssim$ 2 GeV/c) and E760 (down from 8.9 GeV/c with difficulty, say to 6.5-7 GeV/c). This intermediate momentum range encompasses not only a number of charmonium states but many more resonances of u, d, s quarks and antiquarks, representing a great extension of light hadron spectroscopy.[5] In addition, recent candidate for exotic states have appeared--*e.g.*, the f(2.2) and U(3.1), and more are to be expected in this region.

The great flexibility of the booster antiproton arrangement can be seen by noting that it could readily carry out practically the entire program envisioned in the recent Fermilab workshop on antimatter physics at low energies.[6]

References

1. P. Lefevre, D. Mohl, and D.J. Simon, Ref. 6, p.69.
2. B.E. Bonner and L.S. Pinsky, Ref. 6, p. 457.
3. R. Landua, Ref. 6, p. 36.
4. P.A. Rapidis, Ref. 6, p. 84.
5. D.C. Peaslee, EP&S Division Tech. Note 107, BNL (May, 1984).
6. Proc. 1st Workshop on Antimatter Physics at Low Energy, Fermi National Accelerator Laboratory (April, 1986).

APPENDIX 8

Details of Cost Estimates

A. Pendzick

C' Option

	Cost (K$)	Labor (MW)
Proton Transport		
New C3D2:	80	13
Relocate C3P2, C3QS, C3Q9 & C3P3	15	52
Relocate C' Target Station		10
Remove LESB II		32
Target Region		
Q1 - Q5 magnets & PS available	150	155
D1 - D5 magnets & PS available	475	155
Power, water, shielding available from LESB II		
Instrumentation	30	20
Vacuum	75	10
Building available from GPP	___	___
Total	825	447

Cost Estimates (continued)

	Cost (K$)	Labor (MW)
p beam transport:		
Q1 - Q6 (doublet) AGS 8Q24 magnets and PS available	24	156
Q7 - Q15 (doublets) SREL 8Q24 magnets available	36	234
Water Q1 - Q6 from EEBA Q7 - Q15 air cooled	75	--
D1 - D7 Trim dipoles	105	21
Power supplies 2 - 300V x 100A	80	10
7 - 20V x 500A	70	14
Housing (30)	150	
Slabs 30	45	
Power 30	30	30
Tray, signals, power feed	125	50
Instrumentation	100	30
Vacuum	100	32
Security + 6000' fence	83	20
Magnet & PS hookup materials	100	--
Final focus at target: 3 quadrupoles	200	30
Total	1323	627

Experimental area:	Cost* (K$)
Building 40' x 60' x 30'	180
5-ton crane	25
Power 2-1/2 MW (new) (extended from the open area)	50

---

* C' line terminates at 800m near RHIC Open Area. (Four O'Clock Hall)

	Cost (K$)	Labor (MW)	Cost* (K$)
Domestic water and cooling tower (extended from RHIC open area)	175		50
Sprinklers, fire detection, etc.	75		75
Telephones, signals, etc.	50	25	50
Totals	755	25	430
GRAND TOTALS	2,903	1,099	2,578
High Resolution Beam Spectrometer**	1,070	300	1,070

---

* C' line terminates at 800m near RHIC Open Area (Four O'Clock Hall)

** Assuming quadrupoles are available.

U-Line Option

	Cost (K$)	Labor (MW)
Slow Extraction from AGS:	500	186
Proton transport in U-line:		
UQ10 available	15	13
UQ11 available	15	13
UQ12 (N3Q48)	95	31
Trim Doublet	30	26
Water, power, power supplies available	___	___
Total	155	83
Target Region:		
Shielding - 1650 tons concrete	495	--
200 tons steel @ 500/	100	--
Civil contracts	225	--
U-Target and instrumentation	35	10
Q1	95	31
Q2	30	31
D1	95	31
Vacuum	30	10
Total	1105	113
$\bar{p}$ beam transport		
To RHIC injection area (not part of this estimate)		
Vertical bends: 2 - 3X12D75	190	62
200' beam transport: 7 - 4" quads	280	217
Power supplies - 2	80	10
Tunnel extension 100'	200	
Trays, signals, power	75	25

	Cost (K$)	Labor (MW)
Magnet and PS hookup materials	35	
Vacuum	30	10
Instrumentation	20	10
Quad houses and slabs - 3	20	
Final focus at target - 3 quads	200	30
Total	1130	364
Experimental area:		
Power and water come from the RHIC compressor room at an additional cost of $25K.	455	25
GRAND TOTAL	3345	771

D/U Option - Transfer to "U" Line

	Cost (K$)	Labor (MW)
Proton Transport:		
New DQ5	95	13
New DQ6	95	13
Total	190	26
Target Region:		
"D" Target	35	10
Q1	95	31
Q2	30	31
D1 - D4	380	124
Beam port through ring wall	35	12
Water, power and power supplies available		
Vacuum	50	10
Instrumentation	25	10
Total	650	228
$\bar{p}$ beam transport:		
200' to 4-1/2° bend in U-line: 7 quads	280	217
Match to 4-1/4° bend: 2 - 18D36	190	62
New UD1	95	31
To RHIC injection area (not part of this estimate)		
Vertical bends: 2 - 3X12D72	190	62
200' beam transport: y - 4" quads	280	217
Power supplies - 5	200	
100' tunnel extension	200	
Tray, signals, power	75	25

	Cost (K$)	Labor (MW)
Magnet & power supply hookup materials	65	
Vacuum	50	20
Instrumentation	20	10
Quad houses and slabs - 3	20	
Final focus at target 3 quads	200	30
Total	1,865	656
Experimental area:		
Power and cooling water come from the RHIC compressor room at additional cost of $24K	455	25
GRAND TOTAL	3,160	935

D/g-2 Option

	Cost (K$)	Labor (MW)
Proton transport:		
New D110	95	31
New DQ11	95	31
Total	190	62
Target region:		
"D" target	35	10
Q1	95	31
D1	95	31
Power, water, shielding available		
Vacuum	25	6
Instrumentation	25	10
Total	275	119
$\bar{p}$ beam transport:		
1400' like C' option $\frac{1400}{3000}$ x 1123K	524	279
Final focus at target - 3 quads	200	30
Total	724	309
Experimental area:		
Same as 800m variant of C' option except power and water come from RHIC compressor room at an additional cost of $25K	455	25
GRAND TOTAL	1644	515

D/(g-2)' Option

	Cost (K$)	Labor (MW)
Proton transport:		
Same as above for D/(g-2)	190	62
Target region:		
Same as above for D/(g-2)	275	119
$\bar{p}$ beam transport:		
1625' at C' option rate	608	324
20° bend - 4 dipoles and PS	540	132
Final focus at target - 3 quads	200	30
Total	1348	486
GRAND TOTAL	1813	667

Booster Option

	Cost (K$)	Labor (MW)
Target region:		
Lithium lens	250	?
D1	95	31
Q1	95	31
Q2		
Power supplies available		
Shielding - 900t concrete	270	
Vacuum	30	20
Instrumentation and target station	35	10
Power and water relocation	75	
Total	945	123
$\bar{p}$ transport to booster:		
50° bend: 4 - 18D72	380	124
416' beam transport at C' rate	156	83
Quad dipoles to match into booster - 5	200	155
Power supplies - 8	280	16
Total	1016	378
Booster modifications:		
Ejection line (30')	90	12
Ejection equipment	175	60
Booster tunnel modifications:		
New HI line	50	16
Widen 1/6 of existing tunnel	75	10
Booster magnet modifications to reach 6.3 GeV/c	600	186
Total	990	284

	Cost (K$)	Labor (MW)
Transport to 80" bubble chamber building:		
416' beam transport at C' rate	156	83
Dipoles and PS - 2	270	62
Final focus at target - 3 quads	200	30
Total	626	175
Experimental area:		
80" Bubble Chamber addition building 40' x 60' x 30'	180	
Extend 40-ton crane range	25	
Power (2.5 MW)g-2)	50	
Domestic Water	50	
Sprinklers, fire detection etc.	75	
Telephones, signals, etc.	50	25
Total	430	25
GRAND TOTAL	4107	985